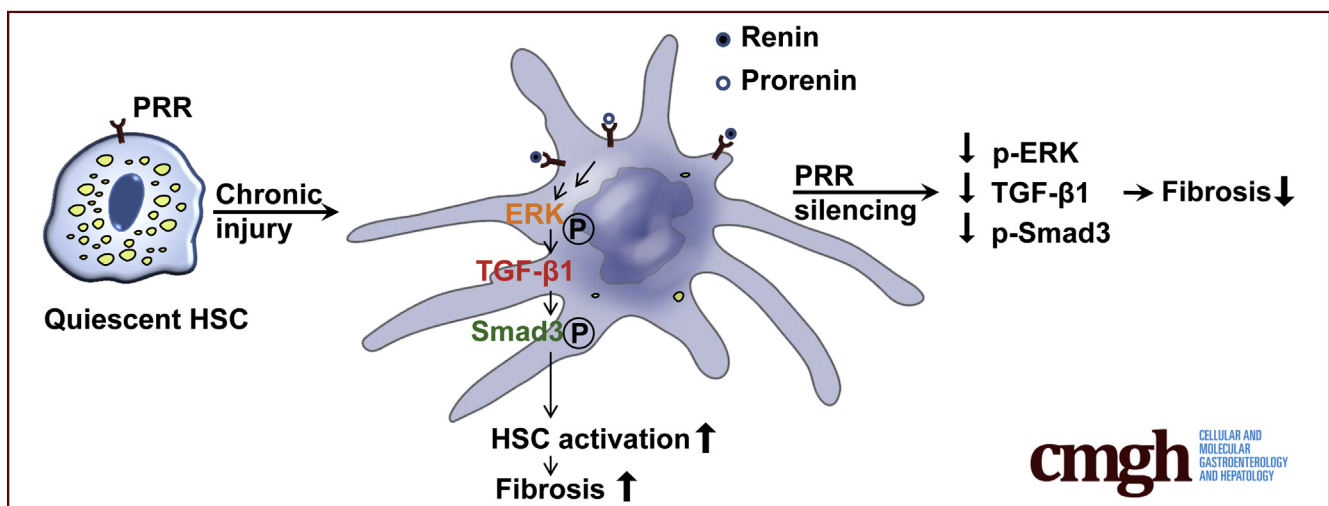


## ORIGINAL RESEARCH

(Pro)renin Receptor Knockdown Attenuates Liver Fibrosis Through Inactivation of ERK/TGF- $\beta$ 1/SMAD3 Pathway

Yun-Cheng Hsieh,<sup>1,2,3</sup> Kuei-Chuan Lee,<sup>1,2</sup> Hao-Jan Lei,<sup>2,4</sup> Keng-Hsin Lan,<sup>1,2,3</sup> Teh-la Huo,<sup>1,2,3</sup> Yi-Tsung Lin,<sup>2,5</sup> Che-Chang Chan,<sup>1,2</sup> Bernd Schnabl,<sup>6</sup> Yi-Hsiang Huang,<sup>1,2</sup> Ming-Chih Hou,<sup>1,2</sup> and Han-Chieh Lin<sup>1,2</sup>

<sup>1</sup>Division of Gastroenterology and Hepatology, <sup>5</sup>Division of Infectious Disease, Department of Medicine, <sup>4</sup>Division of General Surgery, Department of Surgery, Taipei Veterans General Hospital, Taipei, Taiwan; <sup>2</sup>Department of Medicine, <sup>3</sup>Institute of Pharmacology, National Yang-Ming University School of Medicine, Taipei, Taiwan; <sup>6</sup>Department of Medicine, VA San Diego Healthcare System, San Diego, California



## SUMMARY

(Pro)renin receptor is up-regulated in human and mouse fibrotic livers, and in activated hepatic stellate cells. Knockdown of (pro)renin receptor in the liver or specifically in myofibroblasts mitigates liver fibrosis and hepatic stellate cell activation in animal models.

**BACKGROUND & AIMS:** Activation of the (pro)renin receptor (PRR) up-regulates the expression of profibrotic genes in the kidney and heart. We aimed to investigate the role of PRR in hepatic fibrogenesis.

**METHODS:** Human hepatic PRR levels were measured in patients with or without liver fibrosis. PRR expression was analyzed in primary mouse hepatic stellate cells (HSCs). Experimental fibrosis was studied in thioacetamide (TAA)-treated or methionine choline-deficient (MCD) diet-fed C57BL/6 mice. Lentivirus-mediated PRR short hairpin RNA was used to knockdown hepatic PRR expression. Lentiviral vectors expressing PRR short hairpin RNA or complementary DNA from the  $\alpha$ -smooth muscle actin promoter were used for myofibroblast-specific gene knockdown or overexpression.

**RESULTS:** PRR is up-regulated in human and mouse fibrotic livers, and in activated HSCs. Hepatic PRR knockdown reduced liver fibrosis by suppressing the activation of HSCs and expression of profibrotic genes in TAA or MCD diet-injured mice without significant changes in hepatic inflammation. Renin and prorenin increased the expression of PRR and production of TGF- $\beta$ 1 in human activated HSC Lieming Xu-2 cells, and knockdown of PRR inactivated Lieming Xu-2 cells with decreased production of transforming growth factor (TGF)- $\beta$ 1 and Mothers against decapentaplegic homolog 3 (Smad3) phosphorylation. Myofibroblast-specific PRR knockdown also attenuated liver fibrosis in TAA or MCD diet-injured mice. Mice with both myofibroblast-specific and whole-liver PRR knockdown showed down-regulation of the hepatic extracellular signal-regulated kinase (ERK)/TGF- $\beta$ 1/Smad3 pathway. Myofibroblast-specific PRR overexpression worsened TAA-induced liver fibrosis by up-regulating the ERK/TGF- $\beta$ 1/Smad3 pathway.

**CONCLUSIONS:** PRR contributes to liver fibrosis and HSC activation, and its down-regulation attenuates liver fibrosis through inactivation of the ERK/TGF- $\beta$ 1/Smad3 pathway. Therefore, PRR is a promising therapeutic target for liver fibrosis. (*Cell Mol Gastroenterol Hepatol* 2021;12:813–838; <https://doi.org/10.1016/j.jcmgh.2021.05.017>)

**Keywords:** Hepatic Stellate Cell; Gene Targeting; Chronic Liver Disease; Molecular Mechanisms.

Hepatic fibrosis results from chronic liver injury caused by viral infection, alcohol abuse, metabolic disorder, or immune attack. Hepatic fibrosis is a critical pre-stage in the development of cirrhosis, which causes severe morbidity and mortality.<sup>1</sup> After chronic injury, the liver undergoes a repair process accompanied by inflammation and accumulation of extracellular matrix. Hepatic stellate cells (HSCs), the major collagen-producing cells, are responsible for liver fibrosis.<sup>2</sup> Damaged hepatocytes release inflammatory cytokines that activate Kupffer cells (KCs) and recruit inflammatory immune cells, which in turn secrete cytokines, chemokines, and reactive oxygen species to stimulate the activation of resident HSCs from a quiescent state into myofibroblast-like cells, thereby acquiring proliferative, proinflammatory, and fibrogenic properties.<sup>3,4</sup> In addition, the hepatocytic apoptotic bodies resulting from various injuries are engulfed by KCs and HSCs, thereby promoting the expression of profibrogenic proteins.<sup>5</sup> Activated HSCs up-regulate interstitial collagen production, increase synthesis of tissue inhibitor of metalloproteinase-1 (TIMP1), and decrease the production of fibrolytic metalloproteinases, leading to liver fibrosis.<sup>3,4</sup> Besides the treatment of underlying liver diseases, new antifibrotic drugs are being developed to target liver metabolism, apoptosis, inflammation, and fibrosis remodeling. Nevertheless, only a minority of patients achieve treatment response.<sup>6</sup> Therefore, novel effective and safe antifibrotic treatments are needed urgently.

(Pro)renin receptor (PRR), also known as adenosine triphosphatase H(+)-transporting lysosomal accessory protein 2, is a newly identified single-pass transmembrane protein encoded by the *ATP6AP2* gene in human beings, which is expressed in a variety of organs, including the heart, brain, placenta, kidneys, and liver.<sup>7,8</sup> Binding of PRR to renin or prorenin increases the catalytic efficiency for angiotensin II generation<sup>7,8</sup> and directly triggers intracellular signal transduction, leading to activation of extracellular signal-regulated kinase 1 and 2 (ERK1/2) by an angiotensin II-independent mechanism, thereby up-regulating the expression of profibrotic genes such as transforming growth factor (TGF)- $\beta$ 1, fibronectin, collagen I, and plasminogen activator inhibitor 1 (PAI-1).<sup>9,10</sup> PRR has been shown to contribute to fibrosis in the heart and kidney.<sup>11,12</sup> Levels of serum-soluble PRR correlate with the severity of glomerulosclerosis in patients with nephritis.<sup>12</sup> In *in vitro* studies, renin increased mesangial cell TGF- $\beta$ 1 and matrix protein production through a PRR-mediated mechanism.<sup>10</sup> These findings provide new insights into the role of PRR in tissue remodeling.

Although PRR is expressed in the liver,<sup>7</sup> its role in hepatic fibrogenesis has not been investigated. In this study, we investigated the role of PRR in liver fibrosis by targeting PRR in the liver, specifically in the HSCs. Our data suggest that PRR contributes to hepatic fibrogenesis, and inhibition

of PRR signaling represents a potentially novel therapeutic strategy in the regression of liver fibrosis.

## Results

### *(Pro)renin Receptor Is Up-regulated in Human and Mouse Fibrotic Livers and in Activated HSCs*

To examine whether PRR has a role in liver fibrosis, we first measured the PRR expression in the livers of patients with chronic fibrosis. As shown in **Figures 1A** and **2A**, hepatic PRR protein levels were significantly higher in patients with fibrosis and increased with fibrosis progression. Plasma renin levels also were higher in patients with liver fibrosis (**Figure 1B**). PRR expression was barely detectable in nonfibrotic human liver, but was more abundant in fibrotic areas in the fibrotic human livers, and PRR immunostaining co-localized predominantly with that of  $\alpha$ -smooth muscle actin ( $\alpha$ -SMA) (**Figure 1C**).

To further confirm the link between PRR and liver fibrosis, we used a fibrosis animal model. In the liver of mice treated with thioacetamide (TAA) for 8 weeks, PRR expression level was up-regulated significantly (**Figure 1D**). Given that the expression of PRR has not been studied in liver cells, we isolated primary cells from normal mouse livers and found that PRR was expressed in hepatocytes and nonparenchymal cells (**Figure 2B**). To specify the location of PRR up-regulated in response to fibrotic stimuli, hepatic PRR expression was examined by immunofluorescence; the fluorescence intensity of PRR was augmented markedly in fibrotic liver, and found to mostly co-localize with  $\alpha$ -SMA (**Figure 1E**), as a positive control, PRR immunofluorescence in mouse kidney is shown in **Figure 2C**. Because activated HSCs play a key role in the development and progression of liver fibrosis, we analyzed the transcriptional changes of PRR that occur during HSC activation in mouse-derived primary cultures. A significant increase in the messenger RNA (mRNA) expression of PRR was detected in culture-activated and *in vivo*-activated HSCs isolated from TAA-treated mice compared with quiescent HSCs (**Figure 1F** and **G**).

These data indicate that the expression of PRR is up-regulated in fibrotic liver and highly expressed in activated HSCs.

**Abbreviations used in this paper:** ALT, alanine aminotransferase; DMEM, Dulbecco's modified Eagle medium; ERK1/2, extracellular signal-regulated kinase 1/2; FBS, fetal bovine serum; GFP, green fluorescent protein; His, Histidine; HSC, hepatic stellate cell; IL, interleukin; KC, Kupffer cell; LPS, lipopolysaccharide; LX-2, Lieming Xu-2; MCD, methionine choline-deficient; mRNA, messenger RNA; NAFLD, nonalcoholic fatty liver disease; PAI-1, plasminogen activator inhibitor; PCR, polymerase chain reaction; PRR, (pro)renin receptor; SEC, sinusoidal endothelial cell; shRNA, short hairpin RNA; siRNA, small interference RNA; SMA, smooth muscle actin; SMAD3, Mothers against decapentaplegic homolog 3 (Smad3); TAA, thioacetamide; TGF, transforming growth factor; TIMP1, tissue inhibitor of metalloproteinase-1; TNF, tumor necrosis factor.



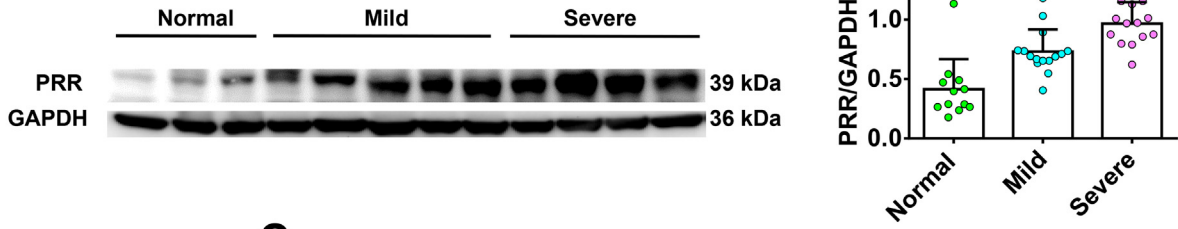
Most current article

© 2021 The Authors. Published by Elsevier Inc. on behalf of the AGA Institute. This is an open access article under the CC BY-NC-ND license (<http://creativecommons.org/licenses/by-nc-nd/4.0/>).

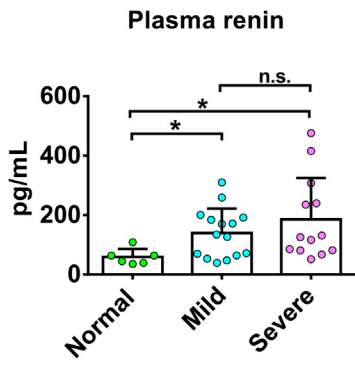
2352-345X

<https://doi.org/10.1016/j.jcmgh.2021.05.017>

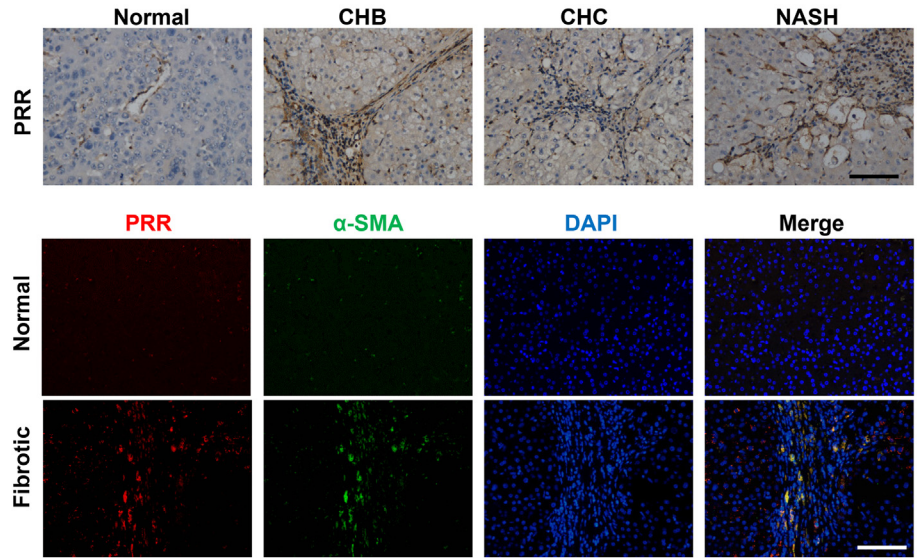
**A**



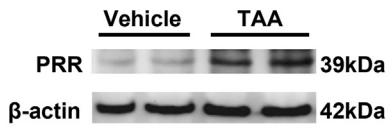
**B**



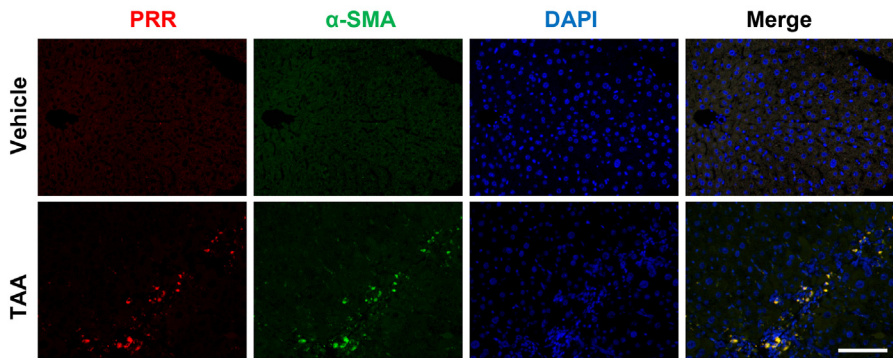
**C**



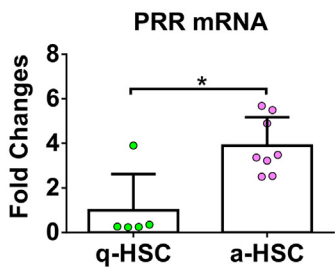
**D**



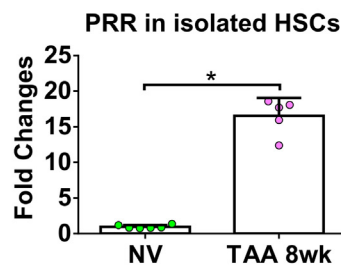
**E**



**F**



**G**



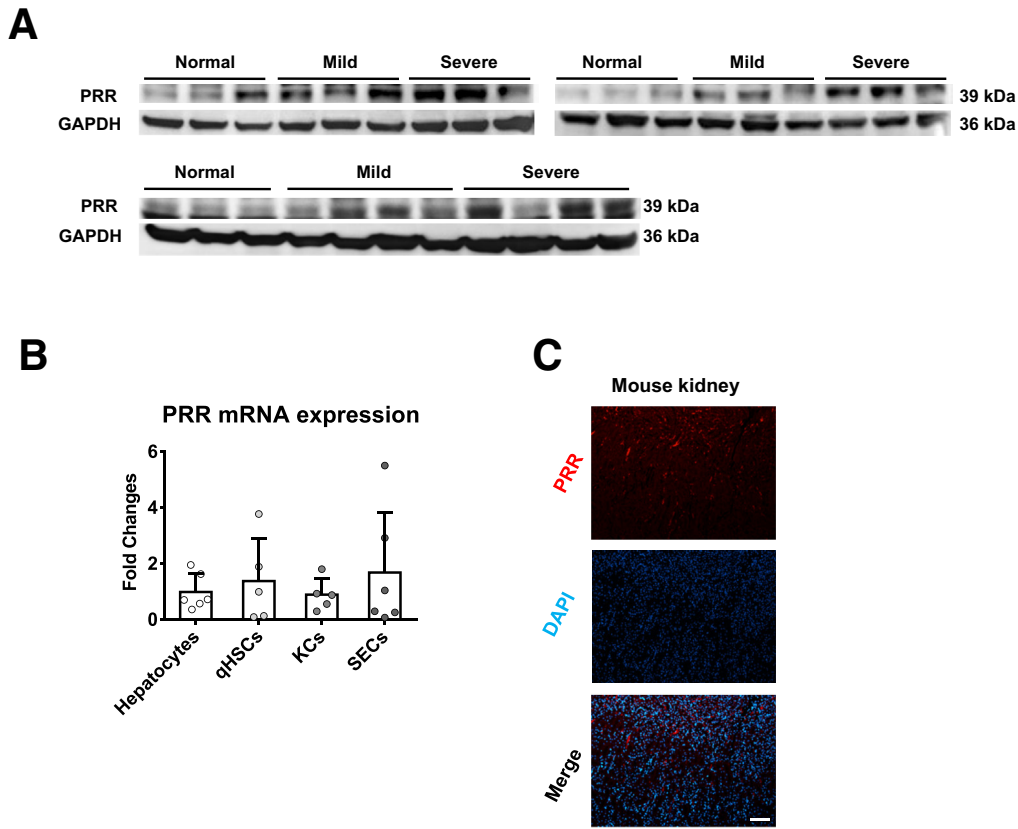


**Figure 2. PRR expression in human livers and mouse primary cells.** (A) Western blot of hepatic PRR from patients without liver fibrosis (normal), and with mild and severe fibrosis (Ishak scores 1~3 and 4~6, respectively). (B) PRR expression in mouse primary hepatocytes, quiescent hepatic stellate cells (qHSCs), KCs, and sinusoidal endothelial cells (SECs) isolated from normal mice (n = 5–6 in each group). (C) PRR immunofluorescence in mouse kidney (PRR, red; diamidino-2-phenylindole [DAPI] nuclear stain, blue). Scale bar: 100  $\mu$ m. GAPDH, glyceraldehyde-3-phosphate dehydrogenase.

### PRR Knockdown Attenuated TAA-Induced Liver Fibrosis

To investigate whether PRR knockdown plays a therapeutic role in liver fibrosis, the effects of PRR knockdown on liver fibrosis were examined. Lentivirus-delivered PRR-specific short hairpin RNA (shRNA) was administered intravenously to inhibit hepatic PRR expression, and a scrambled sequence shRNA was used as a control. PRR shRNA virus significantly suppressed PRR mRNA expression in all isolated primary liver cells (Figure 3).

PRR and scramble-shRNA virus-treated mice showed similar alanine aminotransferase (ALT) levels and severity of liver necroinflammation (Figure 4A and 4B), as well as hepatic expression of proinflammatory cytokines (Figure 4C) after TAA injury. In addition, no significant

alterations were observed in hepatic infiltration of Kupffer cells (KCs), neutrophils, natural killer cells, or invariant nature killer T cells, which were determined by F4/80, myeloperoxidase, Natural killer cell p46-related protein immunostaining, and hepatic Va14Ja18 mRNA expression, respectively (Figure 4D–G).

The effect of PRR knockdown in activated macrophages was investigated using small interference RNA (siRNA) targeting PRR and lipopolysaccharide (LPS) supplementation in the mouse macrophage cell line, RAW 264.7. PRR siRNA significantly inhibited PRR expression in RAW 264.7 cells (Figure 5A). However, the expression of interleukin (IL)1 $\beta$ , IL6, tumor necrosis factor (TNF)- $\alpha$ , and C-C Motif Chemokine Ligand 2 did not decrease after PRR knockdown in these cells (Figure 5B).

**Figure 1. (See previous page). PRR is up-regulated in human and mouse fibrotic livers and in activated HSCs.** (A) *Left:* Representative Western blot of hepatic PRR from patients without liver fibrosis (normal), and with mild and severe fibrosis (Ishak scores 1~3 and 4~6, respectively). The Western blots of hepatic PRR from other patients are shown in Figure 2A. *Right:* Quantification of hepatic PRR expression of the total patients (normal, n = 12; mild fibrosis, n = 15; severe fibrosis, n = 14). \**P* < .05 vs normal group; #*P* < .05 vs mild fibrosis group. (B) Plasma renin levels in patients without liver fibrosis, and with mild and severe fibrosis. \**P* < .05 vs normal group. (C) Immunohistochemical staining for PRR in normal and fibrotic human livers (PRR, red;  $\alpha$ -SMA, green; diamidino-2-phenylindole [DAPI] nuclear stain, blue). (D) Western blot analysis of PRR level in the livers of mice treated with TAA (n = 6) or vehicle (n = 5). (E) Hepatic dual immunofluorescence in TAA mouse fibrosis model (PRR, red;  $\alpha$ -SMA, green; DAPI, blue). (F) mRNA expression of PRR in quiescent (n = 5) and culture-activated (n = 8) HSCs. \**P* < .05 vs quiescent HSC group. (G) mRNA expression of PRR in quiescent HSCs from normal mice treated with vehicle (NV) (n = 6) and in vivo-activated HSCs from TAA-injured mice (n = 5). \**P* < .05 vs NV group. Scale bars: 100  $\mu$ m. a-HSC, activated hepatic stellate cell; CHB, chronic hepatitis B; CHC, chronic hepatitis C; GAPDH, glyceraldehyde-3-phosphate dehydrogenase; NASH, nonalcoholic steatohepatitis; q-HSC, quiescent hepatic stellate cell.

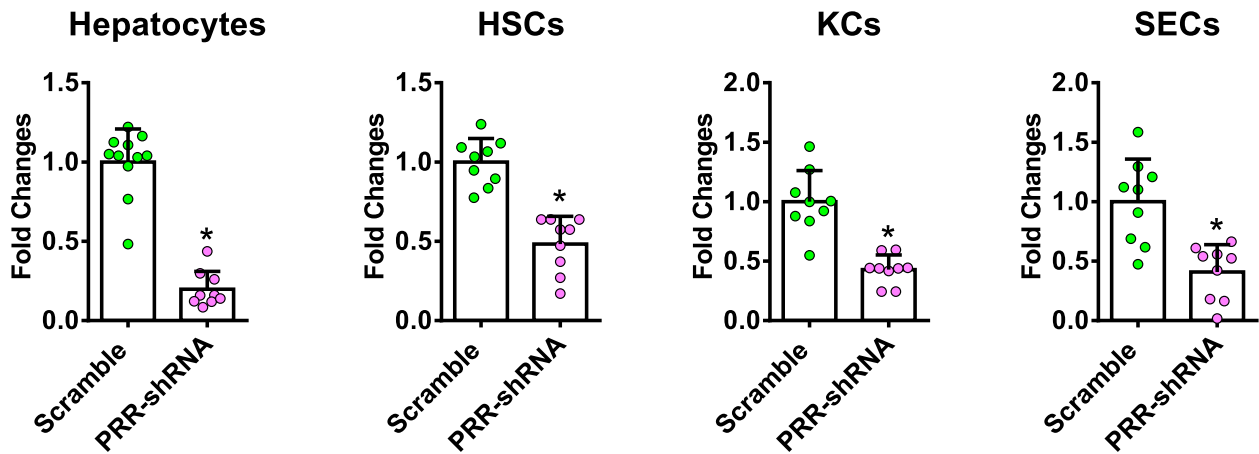


**Figure 3.** PRR mRNA expression of primary liver cells in TAA-injured liver. PRR mRNA expression of primary liver cells isolated from TAA mice treated with lentivirus-delivered scramble or PRR shRNA ( $n = 9-10$  in each group). The expression level in the primary cells isolated from TAA mice treated with scramble virus was assigned arbitrarily as 1.  $*P < .05$  between groups.

PRR shRNA virus successfully knocked down hepatic PRR expression in fibrotic livers (Figure 6A) and reduced PRR co-localization with  $\alpha$ -SMA (Figure 7A). Hepatic renin transcript levels increased after TAA injury, and PRR knockdown modestly reduced the up-regulation of hepatic renin induced by TAA (Figure 6A). Notably, knockdown of PRR attenuated liver fibrosis in TAA-treated mice, as determined by Sirius red staining (Figure 6B) and liver hydroxyproline levels (Figure 6C). The antifibrotic effect of PRR knockdown was supported by the reduction in hepatic  $\alpha$ -SMA expression (Figures 6D and 7B), and transcript levels of collagen 1 $\alpha$ 1, TIMP1, and PAI-1 (Figure 6E).

Because TGF- $\beta$ 1 is a downstream mediator of PRR,<sup>10</sup> the TGF- $\beta$ 1/Mothers against decapentaplegic homolog 3 (Smad3) signaling pathway was investigated to study the mechanism of PRR knockdown in hepatic fibrogenesis. Interestingly, PRR knockdown significantly decreased ERK1/2 phosphorylation, TGF- $\beta$ 1 production, and Smad3 phosphorylation in fibrotic livers (Figure 6F).

These data suggest that the antifibrotic effect of PRR knockdown may be in part through inactivation of HSCs via the down-regulation of the ERK/TGF- $\beta$ 1/Smad3 pathway, and less likely through inactivation of KCs or decreased liver inflammation.

### PRR Knockdown Attenuated Methionine Choline-Deficient Diet-Induced Liver Fibrosis

The antifibrotic effect of PRR knockdown was validated further in a methionine choline-deficient (MCD) diet mouse model. A significant increase in PRR mRNA levels was detected in the in vivo-activated HSCs isolated from 12-week MCD diet-fed mice compared with quiescent HSCs (Figure 8A). Hepatic PRR expression was up-regulated and co-localized with  $\alpha$ -SMA (Figure 8B) in the mice fed with MCD diet. PRR shRNA virus reduced hepatic PRR expression in fibrotic livers (Figure 8C), as well as

liver fibrosis (Figure 8D and E). PRR knockdown also modestly decreased the up-regulation of hepatic renin induced by an MCD diet (Figure 8C). As in the TAA model, PRR shRNA virus reduced hepatic  $\alpha$ -SMA expression (Figure 8F) and transcript levels of collagen 1 $\alpha$ 1 and TIMP1 (Figure 8G). In addition, PRR knockdown attenuated the ERK/TGF- $\beta$ 1/Smad3 pathway in MCD mice (Figure 8H) without significantly altering liver inflammation and steatosis (Figure 9).

### PRR Suppression Inhibited Profibrotic Gene Expression, TGF- $\beta$ 1 Production, and Smad3 Phosphorylation In Vitro

The effect of PRR knockdown was analyzed further in Lieming Xu-2 (LX-2), a human activated HSC cell line. LX-2 cells with PRR knockdown showed reduced expression of profibrotic markers, including PAI-1, and fibronectin (Figure 10A), and decreased ERK1/2 phosphorylation, TGF- $\beta$ 1 expression, and Smad3 phosphorylation (Figure 10B). Moreover, the ligands of PRR, including renin and prorenin, enhanced TGF- $\beta$ 1 production in LX-2 cells (Figure 10C) (LX-2-scramble+renin:  $1.205 \pm 0.074$  vs LX-2-scramble+vehicle:  $1.0 \pm 0.029$ ,  $n = 6/\text{group}$ ,  $P = .002$ ; LX-2-scramble+prorenin:  $1.122 \pm 0.093$  vs LX-2-scramble+vehicle:  $1.0 \pm 0.033$ ,  $n = 10/\text{group}$ ,  $P = .0003$ ), whereas the increase in TGF- $\beta$ 1 production was blocked after PRR knockdown (Figure 10C) (LX-2-shRNA+renin group:  $1.005 \pm 0.117$  vs LX-2-scramble+renin:  $1.205 \pm 0.074$ ,  $n = 6/\text{group}$ ,  $P = .008$ ; and LX-2-shRNA+prorenin group:  $1.035 \pm 0.047$  vs LX-2-scramble+prorenin:  $1.122 \pm 0.093$ ,  $n = 10/\text{group}$ ,  $P = .028$ ). As shown in Figure 10D, renin-induced ERK1/2 phosphorylation was blocked by a specific ERK1/2 inhibitor, U0126, but not altered by a TGF- $\beta$ 1 neutralizing antibody, 19D8. The ERK1/2 inhibitor further blocked TGF- $\beta$ 1 production and downstream SMAD3 phosphorylation (Figure 10E), while the TGF- $\beta$ 1 neutralizing antibody inhibited renin-induced SMAD3

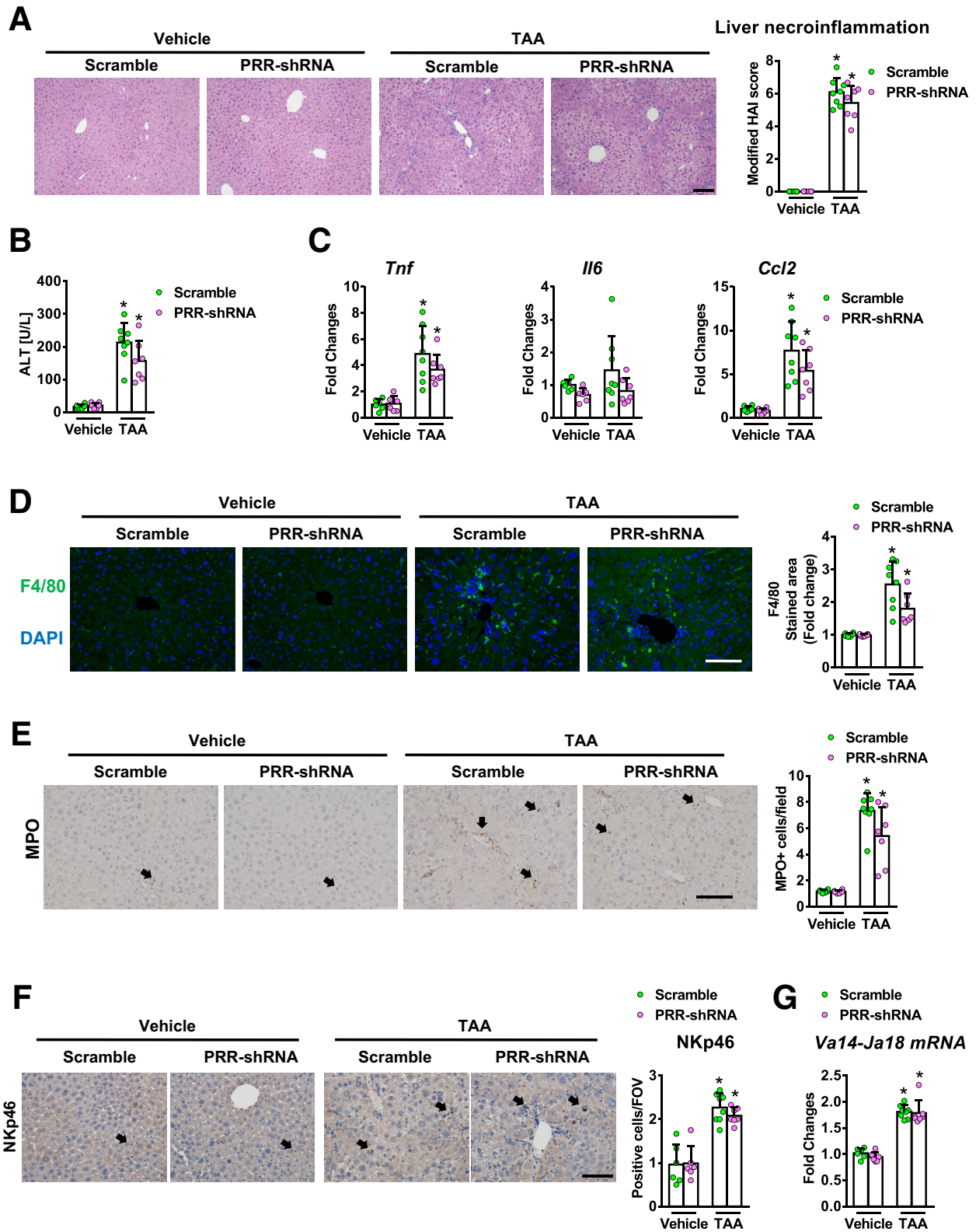


**Figure 4.** Hepatic PRR knockdown did not alter hepatic inflammation in TAA-injured liver. Vehicle or TAA-administered mice were treated with lentivirus-delivered scramble or PRR shRNA ( $n = 6-8$  in each group). (A) Liver necroinflammation was analyzed by H&E staining using a modified Ishak scoring system. (B) Serum ALT levels. (C) mRNA levels of *Tnf*, *Il6*, and *Ccl2*. (D) F4/80 immunostaining of liver sections. (E) Myeloperoxidase (MPO) staining of liver sections. (F) NKp46 immunostaining. (G) Hepatic levels of *Va14-Ja18* mRNA. \* $P < .05$  vs mice treated with vehicle and scramble virus. Scale bar: 100  $\mu\text{m}$ . Arrows indicate positive cells. FOV, field of view.

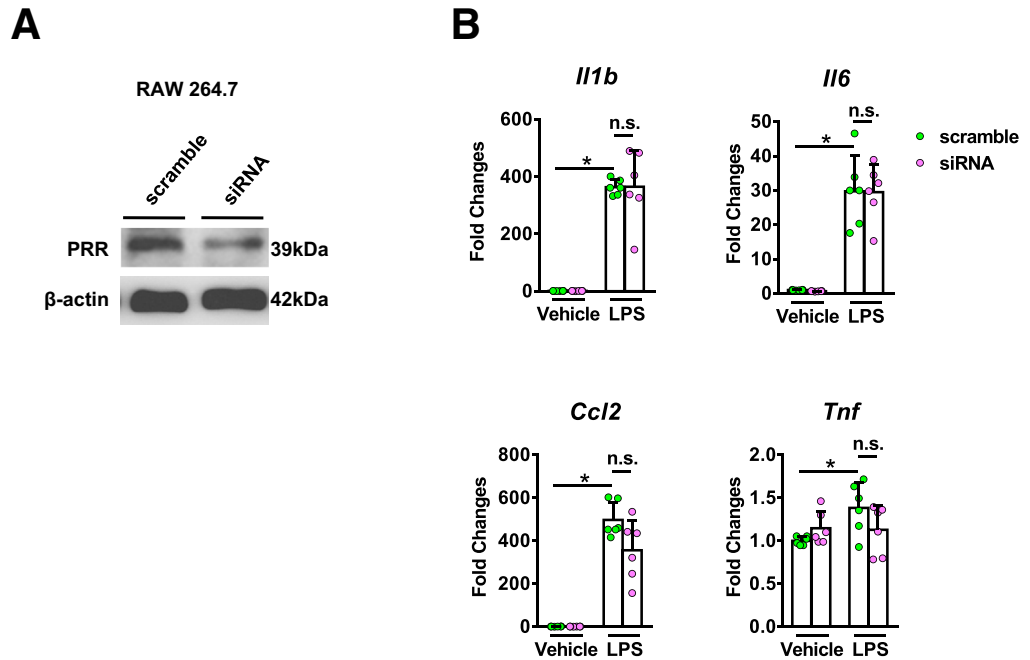


**Figure 5.** The effects of PRR knockdown in RAW 264.7 cells. (A) PRR knockdown in RAW 264.7 cells using siRNA. (B) mRNA expression of *Il1β*, *Il6*, *Tnf*, and *Ccl2* in RAW 264.7 cells treated with LPS (100 ng/mL, 24 h) ( $n = 6$  in each group). \* $P < .05$ .

phosphorylation (Figure 10F). These findings indicate that renin induces up-regulation of the TGF- $\beta$ 1/Smad3 pathway in LX-2 cells via ERK1/2 phosphorylation. Similarly, enhanced expression of the ERK/TGF- $\beta$ 1/Smad3 pathway in human livers with fibrosis progression was observed (Figure 10G).

Next, we investigated whether PRR up-regulation in activated HSCs is regulated by growth factors, cytokines, and PRR ligands. Incubation of LX-2 cells with renin or prorenin induced an increase in the expression of PRR (Figure 10H), consistent with the change in primary mouse activated HSCs (Figure 10I). However, other substances including platelet-derived growth factor composed of two B subunits, TNF- $\alpha$ , TGF- $\beta$ 1, and epidermal growth factor did not enhance the gene expression of PRR (Figure 10H).

#### Myofibroblast-Specific Knockdown of PRR Ameliorated Liver Fibrosis in Mice Treated With TAA or MCD Diet

Given that suppressed PRR expression was observed in all isolated primary liver cells in the hepatic PRR knockdown experiment, we cannot exclude that the antifibrotic effect of PRR knockdown may be mediated partially by hepatocytes, KCs, or sinusoidal endothelial cells (SECs). To focus on the effects of PRR knockdown in activated HSCs/myofibroblasts on liver fibrosis, we further generated a lentiviral construct comprising the gene encoding PRR-specific shRNA within an optimized shRNA-microRNA system,<sup>13</sup> downstream of the  $\alpha$ -SMA promoter (Figure 11A), and the packaged virus vectors were administered to mice. Successful delivery to the myofibroblasts was confirmed in vivo by co-localization of green fluorescent protein (GFP) with  $\alpha$ -SMA-positive cells (Figure 11B) and was verified by GFP expression in isolated HSCs with decreased PRR levels

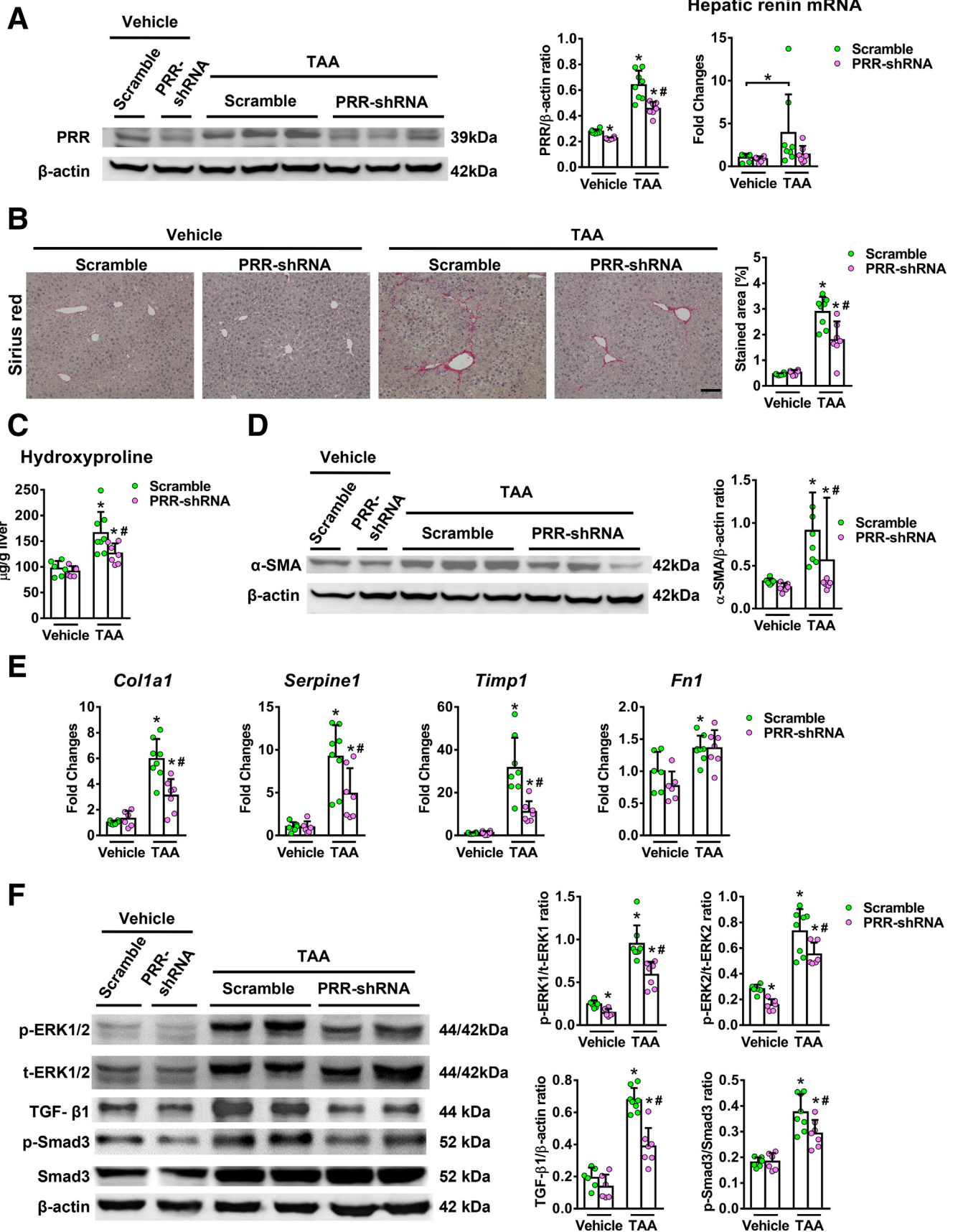
(Figure 11C). Isolated hepatocytes, KCs, and SECs did not show decreased PRR expression levels, indicating myofibroblast-specific knockdown (Figure 12A). In Sirius red staining and hepatic hydroxyproline assay, knockdown of PRR, specifically in myofibroblasts, significantly attenuated TAA-induced collagen deposition (Figure 11D and E). ALT levels (SMA-GFP microRNA [miR]-scramble group:  $232.2 \pm 70.5$  vs SMA-miR-shPRR:  $196.4 \pm 101.0$  U/L;  $P = .18$ ) and hepatic renin mRNA levels (Figure 12B) were similar between the groups.

Moreover, the reduction in hepatic  $\alpha$ -SMA levels (Figure 11F), hepatic transcript expression of collagen 1 $\alpha$ 1, PAI-1, and fibronectin (Figure 11G) in the SMA-miR-shPRR group showed the inhibitory effects of myofibroblast-specific knockdown of PRR on profibrotic factors. In addition, myofibroblast-specific knockdown of PRR down-regulated the ERK/TGF- $\beta$ 1/Smad3 pathway (Figure 11H).

In an MCD diet-induced liver fibrosis model, myofibroblast-specific knockdown of PRR reduced collagen deposition (Figure 13A and B) and hepatic  $\alpha$ -SMA levels (Figure 13C), and down-regulated the ERK/TGF- $\beta$ 1/Smad3 pathway (Figure 13D) without significant changes in serum ALT levels (SMA-miR-scramble group:  $504.4 \pm 175.3$  vs SMA-miR-shPRR:  $18.9 \pm 173.7$  U/L;  $P = .5$ ) and hepatic renin transcript levels (Figure 12C).

#### Myofibroblast-Specific Overexpression of PRR Exacerbated TAA-Induced Liver Fibrosis

Conversely, we examined whether myofibroblast-specific overexpression of PRR aggravates fibrosis in vivo. A lentiviral construct expressing PRR downstream from the  $\alpha$ -SMA promoter was constructed (Figure 14A) and injected into mice. Successful delivery of the histidine (His)-tagged PRR vector to the activated isolated HSCs with the



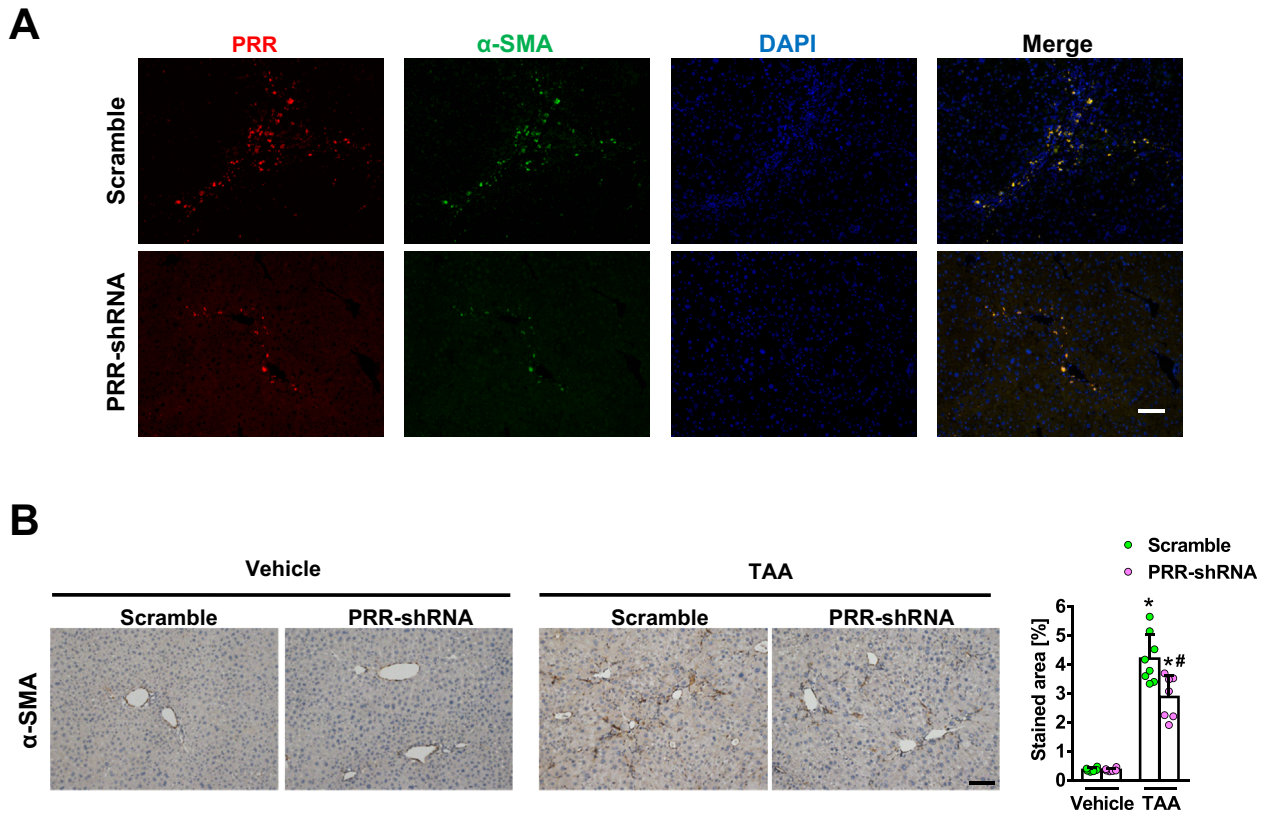


**Figure 7.**  $\alpha$ -smooth muscle actin ( $\alpha$ -SMA) expression in thioacetamide (TAA)-injured liver. Vehicle or thioacetamide (TAA)-administered mice were treated with lentivirus-delivered scramble or PRR shRNA ( $n = 6-8$  in each group). (A) Hepatic immunofluorescence of PRR (red),  $\alpha$ -SMA (green), and DAPI (diamidino-2-phenylindole, nuclear stain, blue) and (B)  $\alpha$ -SMA immunohistochemical staining of liver sections in the 4 groups. \* $P < .05$  vs mice treated with vehicle and scramble virus. # $P < 0.05$  vs mice treated with TAA and scramble virus. Scale bars: 100  $\mu\text{m}$ .

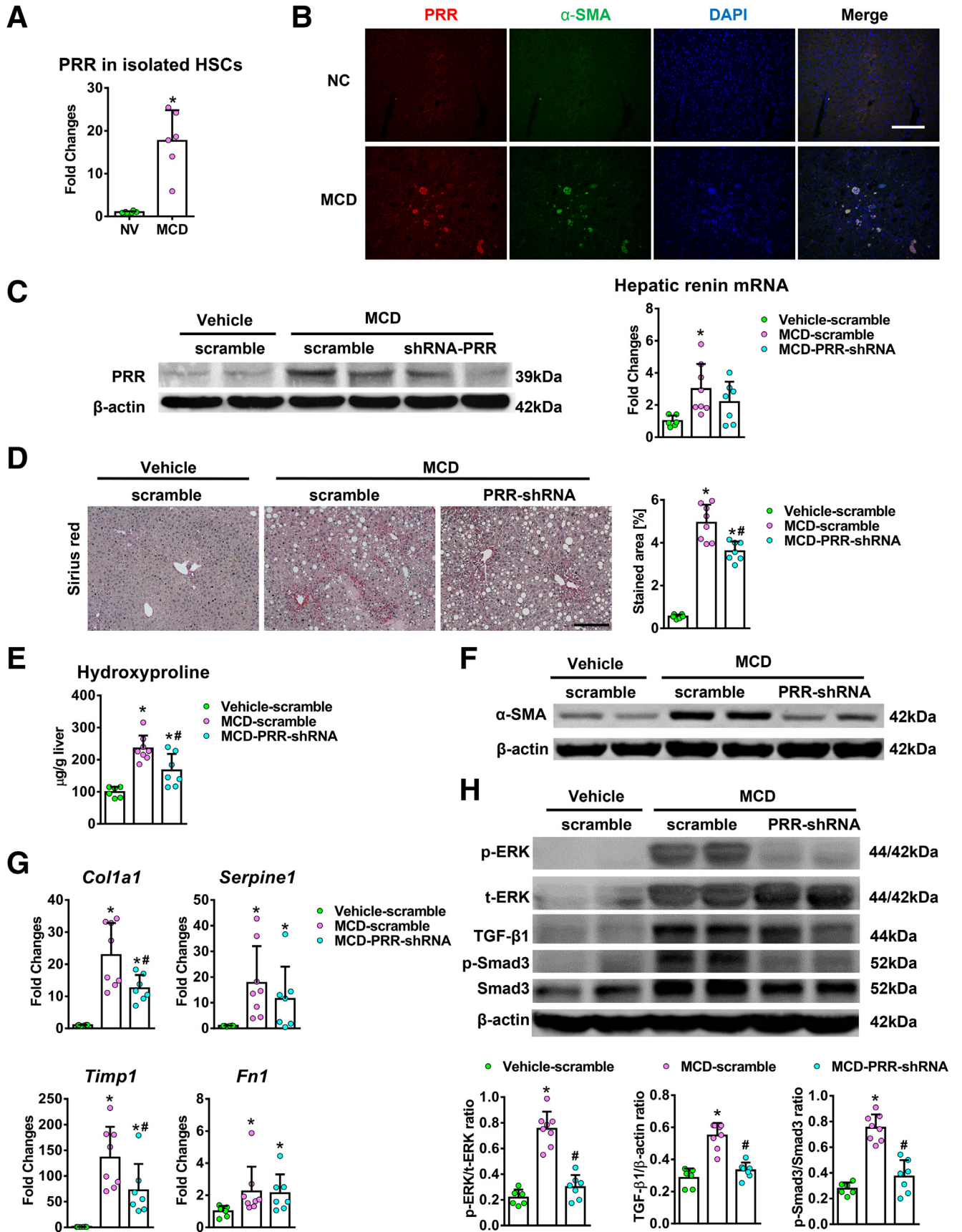
overexpression of PRR was shown (Figure 14B). Hepatic PRR expression was increased after the administration of the SMA-PRR-His virus (Figure 14C). Myofibroblast-specific overexpression of PRR modestly increased hepatic renin transcript levels in TAA-injured mice (Figure 14C). Similar PRR mRNA levels were observed in isolated hepatocytes, KCs, and SECs from SMA-PRR-His and SMA-scramble mice (Figure 12D). Myofibroblast-specific overexpression of PRR significantly aggravated TAA-induced liver fibrosis (Figure 14D and E), with an increase in hepatic collagen 1 $\alpha$ 1, PAI-1, and fibronectin transcript levels (Figure 14F), as well as  $\alpha$ -SMA levels (Figure 14G). In addition, overexpression of PRR in myofibroblasts up-regulated the ERK/TGF- $\beta$ 1/Smad3 pathway in TAA-injured livers (Figure 14G).

## Discussion

In this study, we first showed that PRR expression was increased notably in human and mouse fibrotic livers, and in activated HSCs, and knockdown of PRR induced a marked antifibrotic effect in TAA- and MCD diet-induced mouse models of liver fibrosis with attenuation of HSC activation. The role of the PRR pathway in liver fibrosis, through the activation of HSCs, was shown further in in vitro experiments, and myofibroblast-specific PRR knockdown/overexpression models. These results suggest that therapeutic modulation of PRR is therefore a promising approach for liver fibrosis regression (Figure 15).

Currently, a few novel antifibrotic drugs are being tested in clinical trials targeting liver metabolism, apoptosis, or inflammation with modest efficacy.<sup>6</sup> Because of the complex

**Figure 6.** (See previous page). Hepatic PRR knockdown ameliorated TAA-induced liver fibrosis with suppression of ERK/TGF- $\beta$ 1/Smad3 pathway. Vehicle or TAA-administered mice were treated with lentivirus-delivered scramble shRNA or PRR shRNA ( $n = 6-8$  in each group). (A) Western blot of hepatic PRR levels (left) and expression of hepatic renin mRNA (right) in the 4 groups. (B) Representative images of liver sections after Sirius red staining for the quantification of positively stained area. Scale bar: 100  $\mu\text{m}$ . (C) Hepatic hydroxyproline levels. (D) Western blot of  $\alpha$ -SMA with quantitative analysis. (E) Hepatic transcript expression of *Col1a1*, PAI-1 (*Serpine1*), *Timp1*, and *Fn1*. The expression levels in mice treated with vehicle and scramble virus were assigned arbitrarily as 1. (F) Western blot analysis of phosphorylated and total ERK1/2 (p/t-ERK1/2), TGF- $\beta$ 1, phosphorylated Smad3 (p-Smad3), and Smad3 in mouse livers. \* $P < .05$  vs mice treated with vehicle and scramble virus. # $P < .05$  vs mice treated with TAA and scramble virus.



networks contributing to liver fibrosis, therapeutics against PRR combined with other promising drugs targeting different mechanisms may achieve a synergistic response with better efficacy. Recently, *in vivo* inhibition of type 1 collagen synthesis in HSCs was achieved using collagen 1 alpha 1 (Col1a1) siRNA complexed in lipoplexes.<sup>14</sup> Another study using a vitamin A-coupled liposome to deliver siRNA against a collagen-specific chaperone, heat shock protein-47, showed remarkable specificity in animal models.<sup>15</sup> In our study, the promising results observed with the myofibroblast-specific PRR knockdown in liver fibrosis may be translated into clinical therapeutics through these impressive HSC-targeted approaches in the future.

In this study, knockdown of PRR expression in the whole liver also improved fibrosis without detrimental effects, suggesting the therapeutic potential of PRR antagonists in clinical practice. However, no reliable PRR antagonists currently are available.<sup>16</sup> The first PRR blockers, handle region peptides,<sup>17</sup> have been shown to improve diabetic nephropathy and cardiac fibrosis<sup>11,17</sup>; however, other studies showed conflicting results<sup>18,19</sup> and partial PRR agonistic properties.<sup>20</sup> Another new competitive PRR antagonist, the first 20 amino acids of the prorenin prosegment (PRO20), has been shown to block prorenin-mediated PRR function; however, the effect of PRO20 on blocking renin-mediated PRR activation is unknown.<sup>16</sup> Therefore, a reliable PRR antagonist needs to be developed soon to serve as a possible antifibrotic agent.

PRR was found to be up-regulated in activated HSCs in this study. PRR specifically binds renin and prorenin, and activation of PRR triggers intracellular signal transduction, which activates the ERK1/2 pathway, leading to up-regulation of profibrotic genes, including TGF- $\beta$ 1, PAI-1, collagen, and fibronectin.<sup>9,10</sup> Previous studies have found that intracellular signaling requires minimal binding of PRR, and ERK-1/2 activation was observed with renin and prorenin concentrations as low as 1 pmol/L.<sup>21,22</sup> Bataller et al<sup>23</sup> reported that activation of HSCs *in vivo* and *in vitro* is associated with increased expression of renin. Therefore, in activated HSCs with up-regulated PRR expression, the activation of intracellular PRR signaling, either by circulating renin<sup>24</sup> or locally increased renin production,<sup>23</sup> could be relevant and participate in hepatic tissue remodeling.

In this study, PRR knockdown in LX-2 cells resulted in significant down-regulation of profibrotic genes and decreased TGF- $\beta$ 1 production. TGF- $\beta$ 1 is a potent fibrogenic

cytokine, and HSCs respond to fibrogenic stimuli by producing TGF- $\beta$ 1, which induces phosphorylation of the downstream SMAD proteins, predominantly Smad3, leading to collagen production.<sup>25,26</sup> Previous studies have shown that PRR induces the expression of TGF- $\beta$ 1 and other profibrogenic markers through an ERK-dependent pathway in various renal disease models.<sup>9,10,27,28</sup> The addition of an ERK inhibitor and a neutralizing TGF- $\beta$ 1 antibody, in the current study, confirmed that knockdown of PRR in LX-2 cells led to HSC inactivation by impeding the ERK/TGF- $\beta$ 1/Smad3 pathway. To further confirm the relevance of PRR signaling in HSCs in hepatic fibrogenesis, we generated lentiviral vectors to target PRR in myofibroblasts *in vivo*. Interestingly, myofibroblast-specific PRR knockdown significantly attenuated liver fibrosis in both TAA and MCD diet models with reduced profibrotic gene expression and suppressed the ERK/TGF- $\beta$ 1/Smad3 pathway. These findings were consistent with those of the *in vitro* study. On the other hand, myofibroblast-specific overexpression of PRR aggravated liver fibrosis by up-regulating the ERK/TGF- $\beta$ 1/Smad3 pathway. These findings indicate that PRR in myofibroblasts contributes to the progression of liver fibrosis.

Although PRR also is expressed in KCs and knockdown of PRR in rat mesangial cells attenuated the expression of proinflammatory cytokines,<sup>29</sup> and intravitreal knockdown of PRR with shRNA reduced retinal mRNA expression of IL6, C-C Motif Chemokine Ligand 2, and TNF- $\alpha$  in mice with ocular inflammation,<sup>30</sup> hepatic inflammation was not altered significantly in PRR knockdown mice after TAA or MCD diet-induced injury in the present study. In the *in vitro* experiment, similar expression levels of proinflammatory cytokines and chemokines were noted in PRR or control-siRNA-treated macrophages. Therefore, the results supported the notion that the antifibrotic effects of hepatic PRR knockdown are contributed mainly through the attenuation of HSC activation.

A few studies have shown that PRR inhibition has protective effects for nonalcoholic fatty liver disease (NAFLD),<sup>31,32</sup> and our study further elucidates the role of PRR in mice with NAFLD and liver fibrosis. Ren et al<sup>31</sup> administered N-acetylgalactosamine-modified antisense oligonucleotides in C57BL/6 mice fed a high-fat diet for 14 weeks and found that PRR silencing in hepatocytes for 14 weeks attenuated hepatosteatosis without worsening liver inflammation. In another study, Gayban et al<sup>32</sup> administered PRO-20 for 4 weeks in C57BL/6 mice fed a high-fat diet for

**Figure 8.** (See previous page). **Hepatic PRR knockdown attenuated MCD diet-induced liver fibrosis.** (A) PRR mRNA expression in quiescent HSCs from normal chow (NC)-fed mice and *in vivo*-activated HSCs isolated from mice fed MCD diet for 12 weeks ( $n = 6$  in each group). \* $P < .05$  vs the quiescent HSC group. (B) Hepatic dual immunofluorescence of PRR and  $\alpha$ -SMA in mice fed with NC or MCD diet. Scale bar: 100  $\mu$ m. (C–H) MCD diet-fed mice were treated with lentiviral scramble shRNA or PRR shRNA ( $n = 6$ –8 in each group). Mice fed the NC diet (vehicle) and that received lentiviral-scramble shRNA served as controls ( $n = 6$ ). (C) Western blot analysis of hepatic PRR levels and transcript expression of hepatic renin. (D) Sirius red staining of liver sections and quantification of the positively stained areas. Scale bar: 200  $\mu$ m. (E) Hepatic hydroxyproline levels. (F) Western blot for  $\alpha$ -SMA with quantitative analysis. (G) Hepatic transcript expression of profibrotic genes. The expression levels in the mice treated with vehicle and lentiviral scramble shRNA were assigned arbitrarily as 1. (H) Western blot analysis of phosphorylated and total ERK1/2, TGF- $\beta$ 1, p-Smad3, and Smad3 in mouse livers. \* $P < .05$  vs mice treated with vehicle and scramble virus. # $P < .05$  vs mice fed with MCD diet and scramble virus. DAPI, diamidino-2-phenylindole; NV, normal mice treated with vehicle; p-ERK, phosphorylated extracellular signal regulated kinase; p-SMAD3, phosphorylated SMAD3; t-ERK, total extracellular signal regulated kinase.

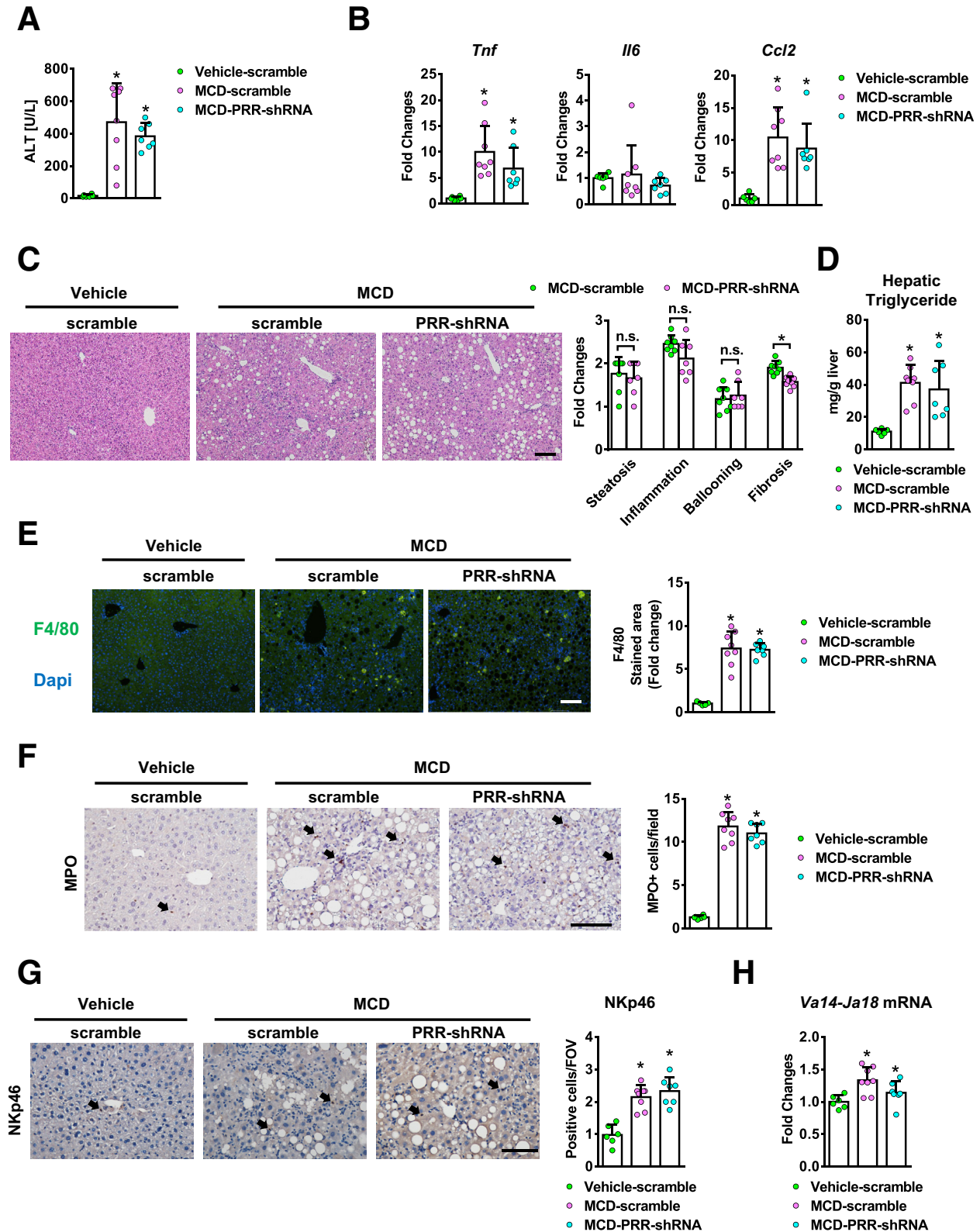


**Figure 9.** Hepatic PRR knockdown did not alter hepatic inflammation in the MCD diet model. The MCD diet–fed mice were treated with lentivirus-delivered scramble or PRR shRNA ( $n = 6–8$  in each group). Mice fed with a normal chow diet (vehicle) and that received scramble virus were served as normal control ( $n = 6$ ). (A) Serum ALT levels. (B) The mRNA levels of *Tnf*, *Il6*, and *Ccl2*. (C) NAFLD scores were analyzed by H&E staining. (D) Hepatic triglyceride levels, and (E) F4/80 immunostaining of liver sections. (F) Myeloperoxidase (MPO) staining of liver sections. (G) NKp46 immunostaining. (H) Hepatic levels of *Va14-Ja18* mRNA. \* $P < .05$  vs mice treated with vehicle and scramble virus. Arrows: positive cells. Scale bar: 100  $\mu\text{m}$ . DAPI, diaminido-2-phenylindole; FOV, field of view.

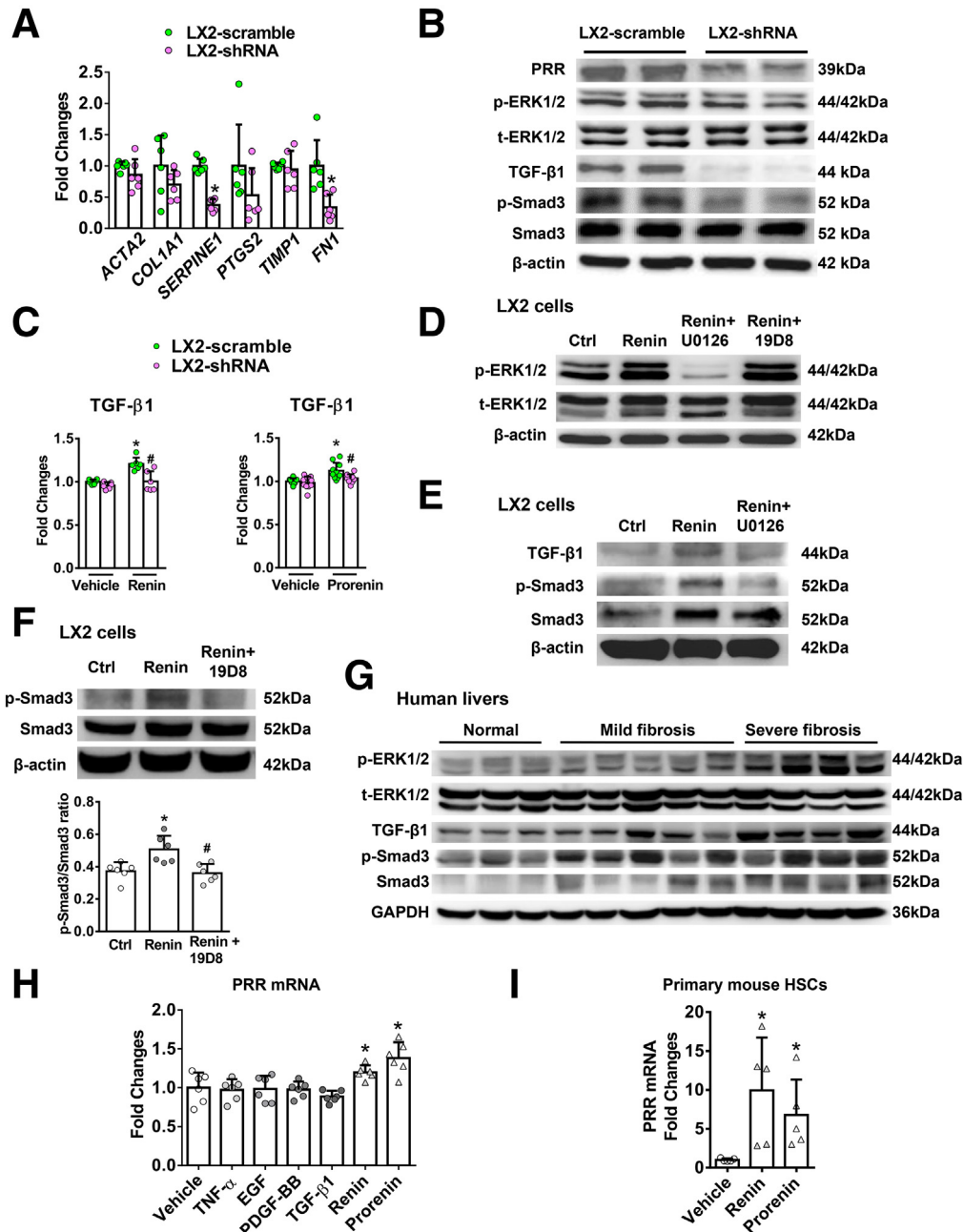


**Figure 10. PRR suppression inhibited expression of profibrotic genes and the ERK/TGF-β1/Smad3 pathway in LX-2 cells.** Knockdown of PRR expression using shRNA reduced the PRR protein level in LX-2 cells (LX-2-shRNA,  $n = 6$ ) compared with scrambled sequences (LX-2-scramble,  $n = 6$ ). (A) mRNA expression of profibrotic genes including *ACTA2*, *COL1A1*, *SERPINE1*, *PTGS2*, *TIMP1*, and *FN1* was analyzed in LX-2 cells with or without PRR knockdown. Significant difference compared with LX-2-scramble cells.  $*P < .05$ . (B) Expression of the ERK/TGF-β1/Smad3 pathway in LX-2 cells with or without PRR knockdown analyzed by Western blot. (C) TGF-β1 production in LX-2-scramble or LX-2-shRNA cells treated with control medium (vehicle), renin ( $10^{-8}$  mol/L) or prorenin ( $10^{-8}$  mol/L) for 24 hours ( $n = 6$ /group for the renin experiment and  $n = 10$ /group for the prorenin experiment). The levels of TGF-β1 were expressed as fold changes relative to the levels of TGF-β1 from LX-2-scramble cells treated with vehicle.  $*P < .05$  vs LX-2-scramble cells treated with vehicle.  $\#P < .05$  vs LX-2-scramble cells treated with renin or prorenin. (D) LX-2 cells were co-incubated with renin ( $10^{-8}$  mol/L), the ERK inhibitor (U0126;  $50 \mu\text{mol/L}$ ), and the TGF-β1 neutralizing antibody (19D8;  $10 \mu\text{g/mL}$ ) for 2 hours. The phosphorylation of ERK was evaluated by Western blot. Ctrl, control cells incubated with vehicle. (E) LX-2 cells were co-incubated with renin ( $10^{-8}$  mol/L) and U0126 ( $50 \mu\text{mol/L}$ ) for 6 hours. The levels of TGF-β1, p-Smad3, and Smad3 were determined by Western blot. (F) LX-2 cells were co-incubated with renin ( $10^{-8}$  mol/L) and 19D8 ( $10 \mu\text{g/mL}$ ) for 6 hours. The phosphorylation of Smad3 was determined by Western blot. (G) Western blot analysis of hepatic ERK/TGF-β1/Smad3 pathway from patients without liver fibrosis (normal), and with mild and severe fibrosis (Ishak scores 1~3 and 4~6, respectively). (H) PRR mRNA expression in LX-2 cells incubated with vehicle, TNF-α ( $100 \text{ ng/mL}$ ), epidermal growth factor (EGF,  $5 \text{ ng/mL}$ ), platelet-derived growth factor-BB (PDGF-BB,  $5 \text{ ng/mL}$ ), TGF-β1 ( $10 \text{ ng/mL}$ ), renin ( $10^{-8}$  mol/L), or prorenin ( $10^{-8}$  mol/L) for 24 hours ( $n = 6$ /group).  $*P < .05$  vs LX-2 cells treated with vehicle. (I) PRR mRNA expression in primary mouse HSCs incubated with renin ( $10^{-8}$  mol/L) or prorenin ( $10^{-8}$  mol/L) for 24 hours ( $n = 5$ /group).  $*P < .05$  vs primary HSCs treated with vehicle. GAPDH, glyceraldehyde-3-phosphate dehydrogenase; p-ERK, phosphorylated extracellular signal regulated kinase; p-SMAD, phosphorylated SMAD; t-ERK, total extracellular signal regulated kinase.

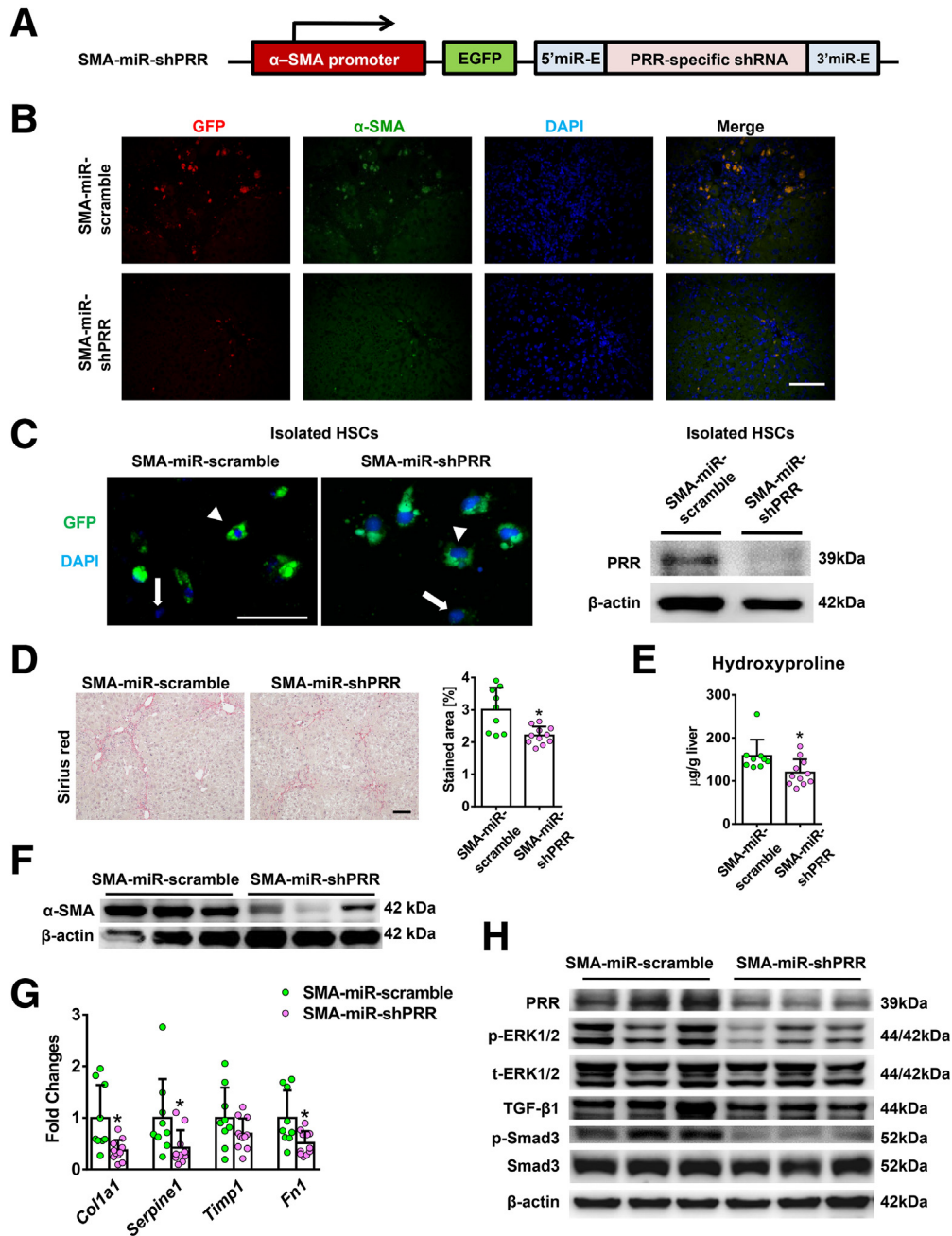


**Figure 11. Myofibroblast-specific knockdown of PRR mitigated liver fibrosis in TAA-injured mice.** Mice administered TAA randomly received injections of lentivirus expressed PRR shRNA ( $n = 11$ ) or scrambled sequences ( $n = 9$ ) under  $\alpha$ -SMA promoter (labeled as SMA-miR-shPRR or SMA-miR-scramble, respectively). (A) Structure of lentiviral SMA-EGFP-miR-PRR shRNA vector. (B) Myofibroblast-specific delivery was confirmed in vivo. Hepatic immunofluorescence of GFP,  $\alpha$ -SMA, and diamidino-2-phenylindole (DAPI). Scale bar: 100  $\mu$ m. (C) HSCs isolated after lentiviral injection, arrowheads indicate GFP (+) cells and arrows indicate GFP (-) cells. Scale bars: 50  $\mu$ m. Western blot analysis of isolated HSCs confirmed successful knockdown of PRR. (D) Sirius red staining of liver sections along with the quantification of positively stained area. Scale bar: 100  $\mu$ m. (E) Hepatic hydroxyproline levels. (F) Western blot analysis of hepatic  $\alpha$ -SMA expression. (G) Hepatic transcript levels of *Col1a1*, PAI-1 (*Serpine1*), *Timp1*, and *Fn1*. The expression levels in mice treated with vehicle and SMA-miR-scramble virus were assigned arbitrarily as 1. (H) Western blot analysis of PRR, phosphorylated and total ERK1/2, TGF- $\beta$ 1, p-Smad3, and Smad3 in mouse livers. \* $P < .05$  vs mice treated with TAA and SMA-miR-scramble virus.

6 weeks and reported that competitive PRR antagonism attenuated the development of hepatosteatosis and portal vein collagen deposition. However, liver inflammation and fibrosis in C57BL/6 mice after being fed a short period of

high-fat diet are minimal.<sup>33</sup> Our study administered lentivirus expressing PRR shRNA into C57BL/6 mice after 6 weeks of MCD diet feeding and down-regulated PRR in hepatocytes, HSCs, KCs, and SECs for 6 weeks and found that

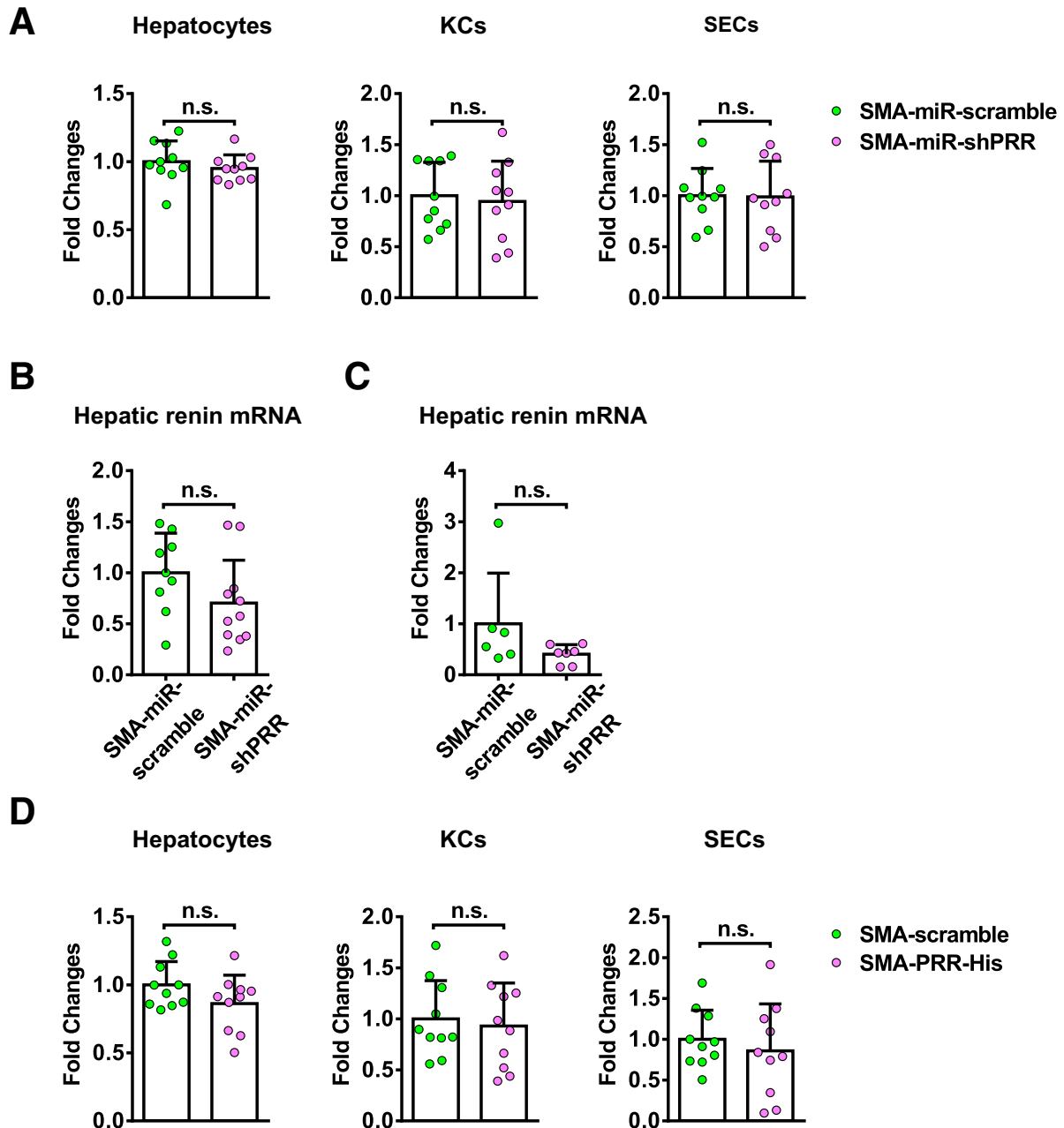


**Figure 12. PRR mRNA expression in primary cells and renin mRNA expression in livers of myofibroblast-specific PRR knockdown mouse models.** (A) PRR mRNA expression in primary hepatocytes, KCs, and SECs isolated from TAA mice treated with SMA-miR-scramble or SMA-miR-shPRR lentivirus ( $n = 10$  in each group). The expression level in the primary cells isolated from TAA mice treated with SMA-miR-scramble virus was assigned arbitrarily as 1. Hepatic renin mRNA expression in (B) TAA-injured mice or (C) MCD diet-fed mice treated with SMA-miR-scramble or SMA-miR-shPRR lentivirus. (D) PRR mRNA expression in primary hepatocytes, KCs, and SECs isolated from TAA mice treated with SMA-scramble or SMA-PRR-His lentivirus ( $n = 10$  in each group). The expression level in the primary cells isolated from TAA mice treated with SMA-scramble virus was assigned arbitrarily as 1.

hepatic PRR knockdown did not reduce hepatosteatosis and liver inflammation; however, it significantly ameliorated nonalcoholic steatohepatitis-related fibrosis, which is the most important prognostic indicator for patients with NAFLD.<sup>34</sup> Our study further showed that myofibroblast-specific PRR knockdown significantly attenuated liver fibrosis in MCD-fed mice and the hepatic PRR expression was up-regulated in patients with nonalcoholic

steatohepatitis. The discrepancy in the antihepatic steatosis effect among the studies may result from different animal models and different methods of PRR inhibition used. Taken together, these studies highlight the different aspects of therapeutic potential of PRR inhibition for NAFLD.

Our study had some limitations. First, global PRR knockout mice or HSC-specific PRR knockout mice are not available, therefore, the effects of PRR modulation for the

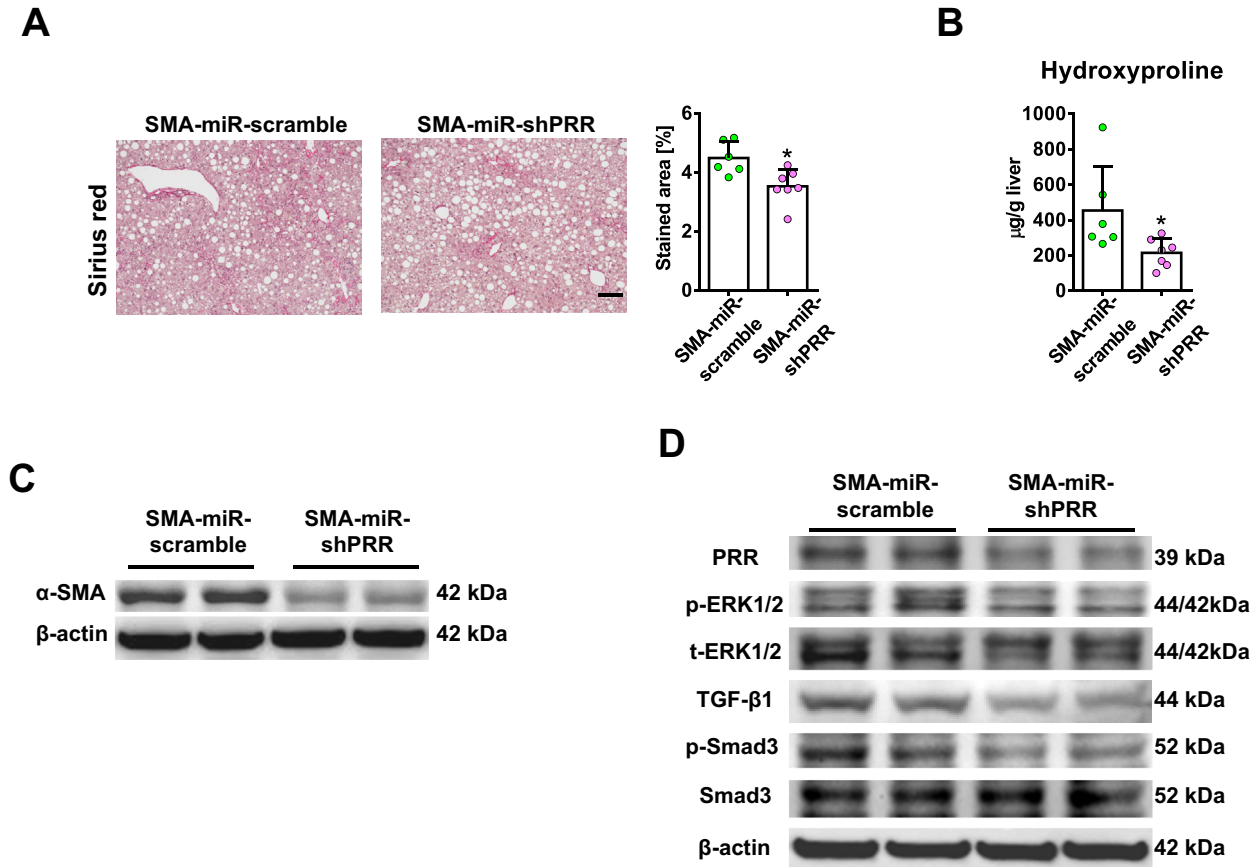


**Figure 13. Attenuation of liver fibrosis by myofibroblast-specific knockdown of PRR in the MCD diet mouse model.** Mice fed with a MCD diet for 6 weeks randomly received injections of lentivirus vector-expressed PRR shRNA ( $n = 6$ ) or scrambled sequences ( $n = 7$ ) under  $\alpha$ -SMA promoter (labeled as SMA-miR-shPRR or SMA-miR-scramble, respectively). All mice were killed after 12 weeks on a MCD diet. (A) Sirius red staining of liver sections with the quantification of the positively stained area. Scale bar: 100  $\mu$ m. (B) Hepatic hydroxyproline contents. (C) Western blot analysis of hepatic  $\alpha$ -SMA levels. (D) Western blot analysis of hepatic the PRR-ERK1/2-TGF- $\beta$ 1-Smad3 pathway. \* $P < .05$  between groups. miR, microRNA; p-ERK, phosphorylated extracellular signal regulated kinase; p-SMAD, phosphorylated SMAD; t-ERK, total extracellular signal regulated kinases.

prevention of liver fibrosis cannot be assessed. However, our models simulate the clinical setting in patients diagnosed with established liver fibrosis, and our results suggest that modulation of PRR is a promising therapeutic approach for fibrosis regression. Second, the effects of pharmacologic inhibition of PRR on liver fibrosis was not investigated in our study. A reliable PRR blocker and HSC-targeted pharmacologic therapeutics for PRR inhibition need to be developed.

In conclusion, our results show the pathophysiology of PRR in liver fibrosis. The promising effect of PRR knockdown in myofibroblasts on liver fibrosis provides evidence for developing a new myofibroblast-targeted therapeutic, which may be combined with other potential antifibrotic drugs for treatment of chronic liver injury.

## Materials and Methods

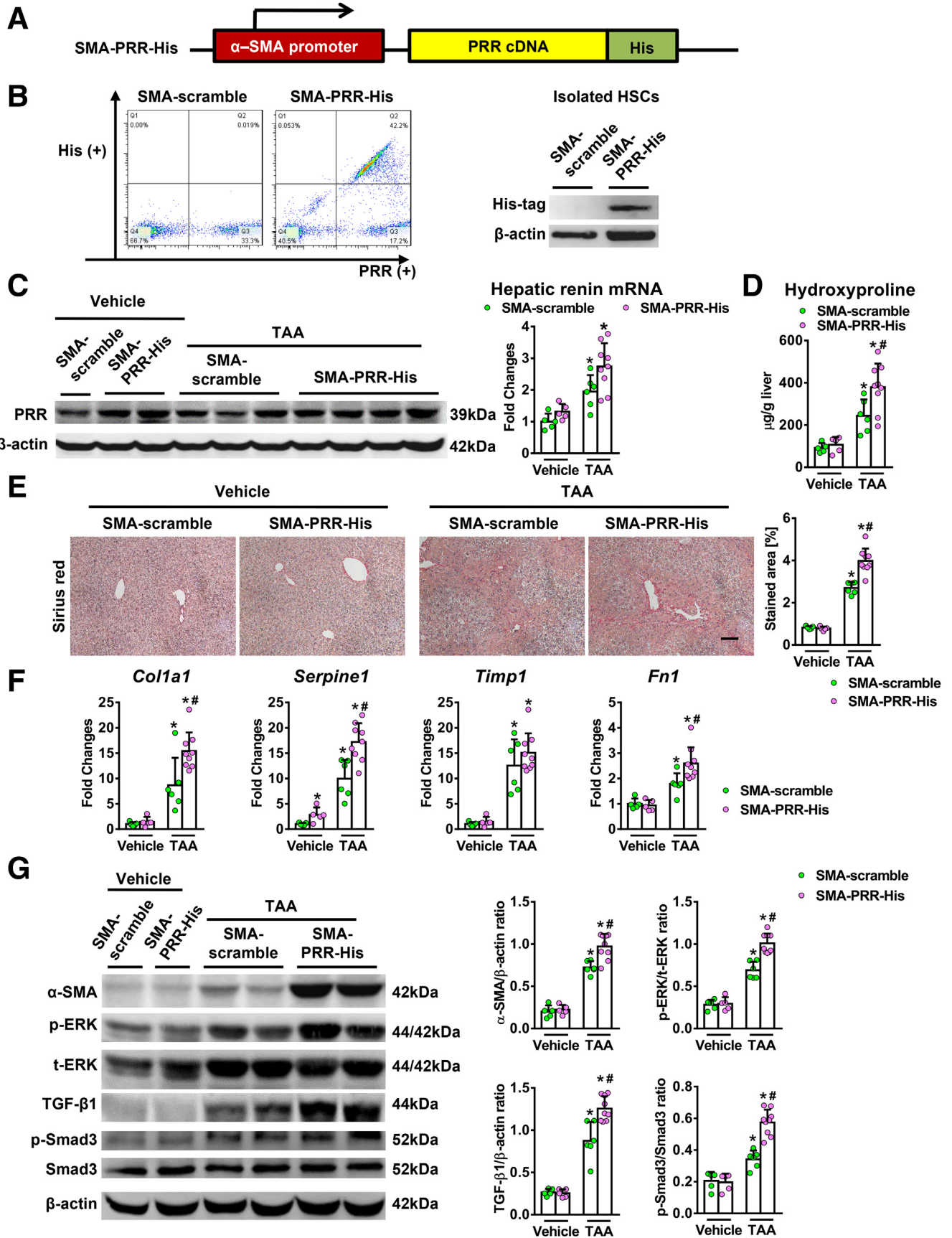
### Human Samples

Nontumorous liver and plasma samples were obtained from 41 patients who underwent surgical liver

resection for hepatocellular carcinoma and were stored at  $-80^{\circ}\text{C}$  until use. Histologic samples were analyzed and classified as nonfibrosis (normal; Ishak score; 0), mild fibrosis (Ishak score, 1–3), or severe fibrosis (Ishak score, 4–6) by the pathologists at Taipei Veterans General Hospital. Demographic data pertaining to the patients are presented in Table 1. Immunohistochemistry and Western blot analyses were performed to analyze the expression of PRR expression as well as the ERK/TGF- $\beta$ 1/SMAD3 pathway. Plasma renin levels were measured using an enzyme-linked immunosorbent assay (Human Renin Enzyme-Linked Immunosorbent Assay Kit, catalog E4719-100; BioVision, Inc, Milpitas, CA). The study protocol was approved by the Institutional Research Board of Taipei Veterans General Hospital (no. 2018-01-015CC).

### Animals

Eight-week-old adult male C57BL/6 mice (National Laboratory Animal Center, Taipei, Taiwan) were used in



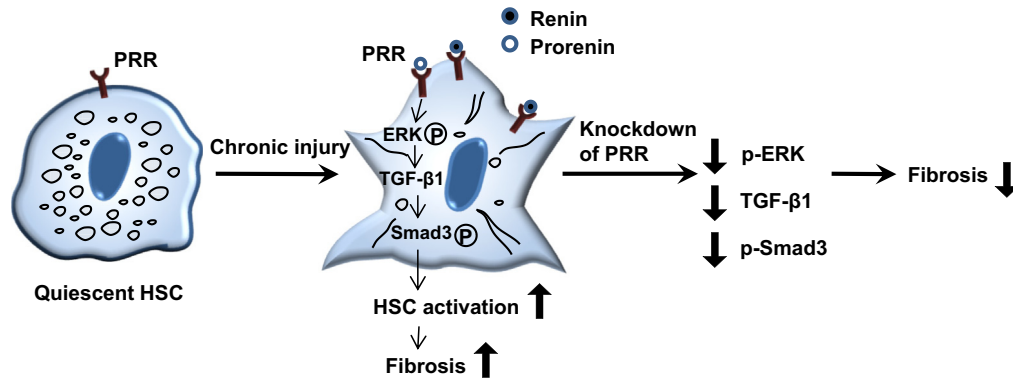


**Figure 15. Schematic of the proposed mechanism of PRR in liver fibrosis.** PRR expression is increased in activated HSCs during chronic liver injury. The binding of renin or prorenin to PRR leads to the activation of the ERK/TGF $\beta$ 1/Smad3 pathway, promoting liver fibrosis. The knockdown of PRR in activated HSCs suppresses the ERK/TGF $\beta$ 1/Smad3 pathway, leading to reduction of liver fibrosis. p-ERK, phosphorylated extracellular signal regulated kinase; p-SMAD3, phosphorylated SMAD3.

each experiment. The mice were caged at 22°C with a 12-hour light-dark cycle and allowed free access to food. The study was approved by the Animal Experiment Committee of Taipei Veterans General Hospital and National Yang-Ming University, and performed in accordance with the Guidelines for the Care and Use of Laboratory Animals prepared by the National Academy of Sciences.

#### Lentivirus Preparation

A shRNA was designed to target the mRNA encoding mouse PRR at the TAATCACCTCTTACAACATTT (NM-027439.3-1002s21c1) sequence. Target and scrambled sequences were ligated and cloned into a lentiviral vector under the control of the U6 promoter. For specific PRR knockdown in myofibroblasts, the ( $\alpha$ -SMA) promoter was amplified from the mouse smooth muscle cell alpha-actin promoter fragment (pSMP8) plasmid, a gift from Dr J. A. Fagin (Memorial Sloan Kettering Cancer Center, New York, NY), using the forward primer 5'-GATCATGATCGAATTCACACCATAAAACAAGTGCATGAG-3' and the reverse primer 5'-GATCATGATCGAATTCAGTGCACCAGCGTCTCAGG-3'.<sup>35</sup> The polymerase chain reaction (PCR) product was cloned into a lentiviral vector with a downstream enhanced GFP. shRNAs target mouse PRR and the scrambled sequence was constructed within a miR-E backbone<sup>13</sup> and cloned downstream of the  $\alpha$ -SMA promoter. For specific PRR overexpression in myofibroblasts, mouse PRR complementary DNA open reading frame clone with C-terminal

His tag (Sino Biological, Inc, Beijing, China) was extracted and cloned downstream of the  $\alpha$ -SMA promoter. The viral construct encoding a scrambled sequence under the  $\alpha$ -SMA promoter served as a control. The constructs were sequenced to verify the orientation and integrity of the inserts. All vectors were constructed and packaged at the RNAi Core Lab (Academia Sinica).

#### Experimental Design

In the hepatic PRR knockdown experiment, liver fibrosis was induced in mice by intraperitoneal injection of TAA (100 mg/kg body weight) 3 times a week for 8 weeks<sup>36</sup> or by feeding the mice a MCD diet for 12 weeks. In the TAA group, lentivirus expressing PRR shRNA or scrambled sequences (100  $\mu$ L of  $1.5 \times 10^7$  transducing units) was administered via tail vein injection after 4 weeks of TAA or vehicle (saline) treatment.<sup>37</sup> All the mice were killed 4 weeks after administration of the lentivirus. In the MCD group, lentivirus with PRR shRNA or scrambled sequences (100  $\mu$ L of  $1.5 \times 10^7$  transducing units) was administered via tail vein injection after 6 weeks of MCD diet feeding. Mice that were fed normal chow diet and received lentivirus with scrambled sequence were served as controls. All mice were killed 6 weeks after the administration of lentivirus.

For the myofibroblast-targeted PRR knockdown experiments, liver fibrosis was induced by intraperitoneal injection of TAA (100 mg/kg body weight) 3 times a week for 8

**Figure 14. (See previous page). Myofibroblast-specific overexpression of PRR aggravated liver fibrosis in TAA-injured mice.** (A) Structure of lentiviral SMA-PRR complementary DNA (cDNA)-His tag vector. (B) HSCs isolated after lentiviral injection. *Left:* Flow cytometric analysis of the expression of His and PRR in HSCs isolated from TAA mice that received SMA-scramble or SMA-PRR-His virus ( $n = 6$  in each group). *Right:* Western blot of the isolated HSCs. (C–G) Vehicle or TAA-administered mice randomly received injections of lentivirus expressing PRR or scrambled sequences ( $n = 5–9$ ) under the  $\alpha$ -SMA promoter (labeled as SMA-PRR-His or SMA-scramble, respectively). (C) Western blot analysis of hepatic PRR levels and hepatic transcript expression of renin. (D) Hepatic hydroxyproline levels. (E) Sirius red staining of liver sections along with the quantification of positively stained areas. Scale bar: 100  $\mu$ m. (F) Hepatic transcript levels of *Col1a1*, PAI-1 (*Serpine1*), *Timp1*, and *Fn1*. The expression levels in mice treated with vehicle and SMA-scramble virus were assigned arbitrarily as 1. (G) Western blot analysis of  $\alpha$ -SMA, phosphorylated and total ERK1/2, TGF- $\beta$ 1, p-Smad3, and Smad3 in mouse livers. \* $P < .05$  vs mice treated with vehicle and SMA-scramble virus. # $P < .05$  vs mice treated with TAA and SMA-scramble virus. p-ERK, phosphorylated extracellular signal regulated kinases; p-SMAD, phosphorylated SMAD; t-ERK, total extracellular signal regulated kinases.

**Table 1.** Patient Characteristics

Variable	No fibrosis (n = 12)	Mild fibrosis (n = 15)	Severe fibrosis (n = 14)	P value
Age, y	61.4 ± 15.8	68.1 ± 9.4	66.4 ± 11.1	.648
Female/male	3/9	5/10	5/9	.831
Ishak score	0	2.1 ± 0.8	4.9 ± 0.9	<.001
Etiology of liver fibrosis	–			.837
ALD		1	2	
ALD + CHB		2	1	
CHB		3	4	
CHC		4	2	
NASH		5	5	

NOTE. Data are expressed as means ± SD.

ALD, alcoholic liver disease; CHB, chronic hepatitis B; CHC, chronic hepatitis C; NASH, nonalcoholic steatohepatitis.

weeks or by feeding the mice an MCD diet for 12 weeks. The mice randomly received lentivirus-expressing PRR shRNA or scrambled sequences under the  $\alpha$ -SMA promoter (labeled as SMA-miR-shPRR or SMA-miR-scramble, respectively) at a dose of 100  $\mu$ L of  $1.5 \times 10^7$  transducing units by tail vein injection after 4 weeks of TAA treatment or 6 weeks of MCD diet. The mice were killed after 4 more weeks of TAA treatment or 6 more weeks of MCD diet, respectively.

In the myofibroblast-specific PRR overexpression experiments, the mice randomly received lentivirus expressing PRR complementary DNA or scrambled sequences under the  $\alpha$ -SMA promoter (labeled as SMA-PRR-His or SMA-scramble, respectively) at a dose of 100  $\mu$ L of  $1.5 \times 10^7$  transducing units via tail vein injection after 4 weeks of TAA or vehicle treatment. The mice were killed after 4 weeks of lentivirus administration.

All the lentivirus vectors themselves did not cause liver inflammation or fibrosis in mouse livers (Figure 16).

### PRR Knockdown in Human Activated HSC LX-2 Cells and In Vitro Experiments

Lentivirus expressing shRNA targeting human PRR mRNA at the sequence GGAACGAGTTTAGTATATTA (NM-005765.2-149s21c1), under the control of a U6 promoter, were constructed by the RNAi Core Lab (Academia Sinica).

To perform lentiviral infection,  $3 \times 10^5$  of LX-2 cells (Merck Millipore, Burlington, MA) were plated in 6-cm plates and incubated overnight at 37°C in 5% CO<sub>2</sub>. On day 2, the medium was replaced with fresh medium containing polybrene (8  $\mu$ g/mL) to enhance lentiviral transfection,<sup>38</sup> and incubated for 30 minutes. Then, the constructed viruses (with a final multiplicity of infection of 3) were added to the medium. After incubation for 24 hours, puromycin (3  $\mu$ g/mL) was added for selection of stable clones and the infected cells were incubated for 72 hours. Protein lysates from the stable clones of PRR knockdown cells and scrambled shRNA-transfected cells were quantified by Western blot to confirm the effect of RNA interference. Cells also were harvested for RNA analysis.

PRR-shRNA-transfected LX-2 and scrambled shRNA-transfected LX-2 cells were treated with recombinant human renin or prorenin (Cayman Chemical, Ann Arbor, MI) at

the indicated dose ( $10^{-8}$  mol/L) and times.<sup>9,10</sup> Culture supernatants were collected, and the level of TGF- $\beta$ 1 was determined by enzyme-linked immunosorbent assay (R&D Systems, Inc, Minneapolis, MN).

Activation of the cellular ERK/TGF- $\beta$ 1/SMAD3 pathway in LX-2 cells was determined by Western blot after treatment with or without 50  $\mu$ mol/L U0126, a specific ERK inhibitor (Cell Signaling, Danvers, MA),<sup>9</sup> or 10  $\mu$ g/mL 19D8, a neutralizing TGF- $\beta$ 1 antibody (BioLegend, San Diego, CA),<sup>39</sup> in the presence of renin ( $10^{-8}$  mol/L) for 24 hours.

The effect of growth factors, cytokines, and PRR ligands on PRR up-regulation in the activated HSCs was analyzed in LX-2 cells incubated with vehicle, TNF- $\alpha$  (100 ng/mL), epidermal growth factor (5 ng/mL), platelet-derived growth factor composed of two B subunits (5 ng/mL), TGF- $\beta$ 1 (10 ng/mL), renin ( $10^{-8}$  mol/L), or prorenin ( $10^{-8}$  mol/L) for 24 hours (n = 6/group).<sup>23</sup>

### Isolation and Culture of Primary Cells

Mouse HSCs, Kupffer cells, and sinusoidal endothelial cells were isolated from male C57BL/6 mice by collagenase–pronase perfusion and subsequent density centrifugation on Nycodenz (Alere Technologies AS, Oslo, Norway) gradient as described previously.<sup>40–42</sup> The purity of the HSCs was tested by retinoid autofluorescence<sup>42</sup> and exceeded 95% in all isolations (Figure 17A). HSCs isolated from normal liver were cultured for 12 hours (quiescent HSCs) or 9 days (culture-activated HSCs) in Dulbecco's modified Eagle medium (DMEM) containing 10% fetal bovine serum (FBS), and antibiotics at 37°C in a humidified atmosphere of 95% air and 5% CO<sub>2</sub>. For in vivo HSC activation, primary HSCs were isolated from mice that were administered intraperitoneal injections of TAA (Sigma, St Louis, MO) (100 mg/kg body weight) for 8 weeks or maintained on a MCD diet for 12 weeks, and cultured in DMEM with 10% FBS and antibiotics for 20 hours (in vivo-activated HSCs). For RNA and protein extraction,  $3 \times 10^5$  HSCs/well were plated in 6-well plates and cultured for the indicated times. To measure mRNA expression of PRR after exposure to PRR ligands, in vivo-activated HSCs from TAA mice were treated with vehicle, renin, or prorenin ( $10^{-8}$  mol/L) for 24 hours.<sup>9,10</sup>

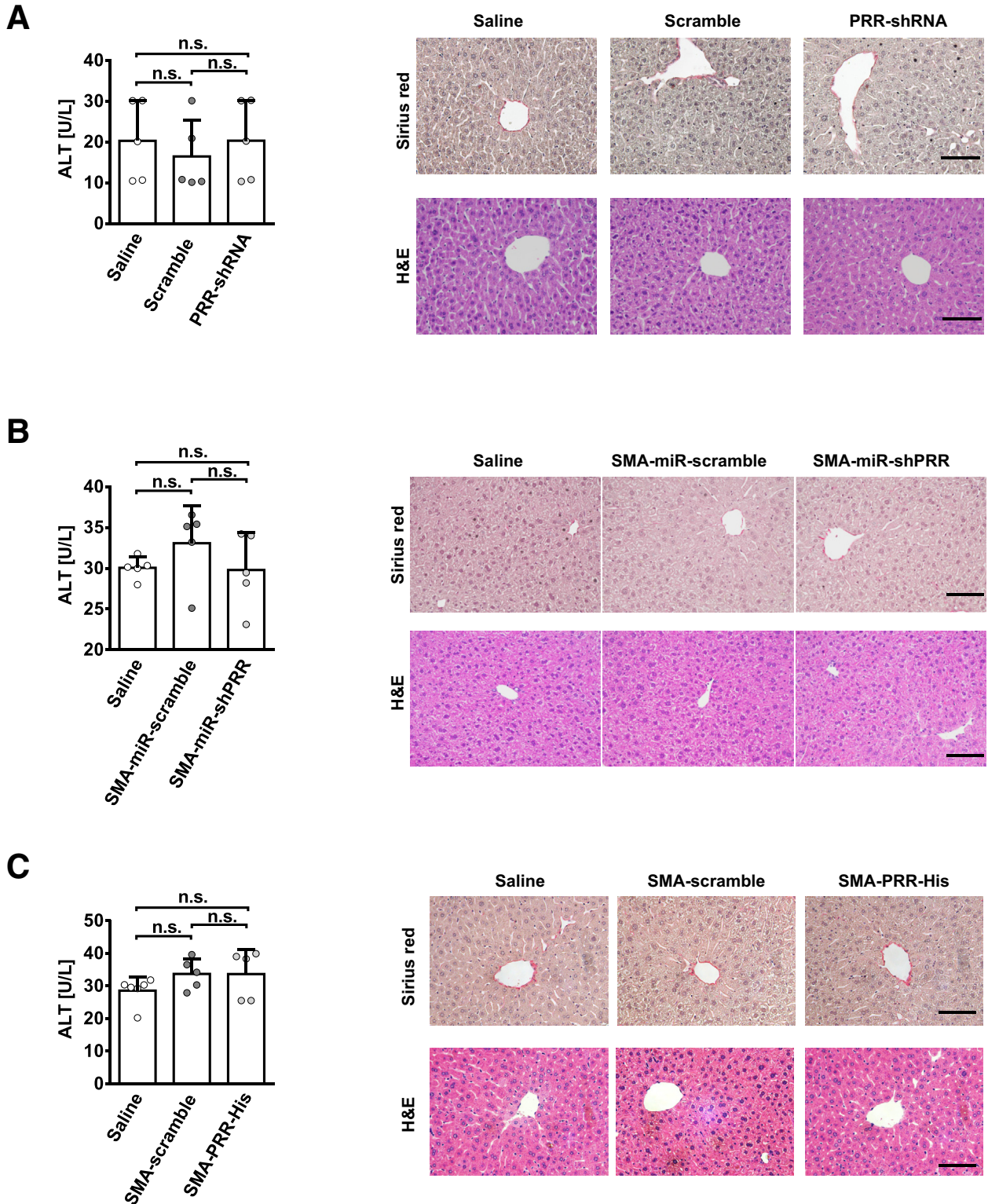


**Figure 16.** Lentiviral vectors did not cause liver inflammation or fibrosis in mice liver. Serum ALT levels, Sirius red staining, and H&E staining of liver in the vehicle-administered mice treated with (A) normal saline, lentivirus-scramble, or lentivirus-PRR-shRNA (killed 4 weeks after injections); (B) normal saline, lentivirus-SMA-miR-scramble, or lentivirus-SMA-miR-shPRR (killed 4 weeks after vector injections); and (C) normal saline, lentivirus-SMA-scramble, or lentivirus-SMA-PRR-His (killed 4 weeks after vector injections). n = 5–6 in each group. Scale bars: 100  $\mu$ m.

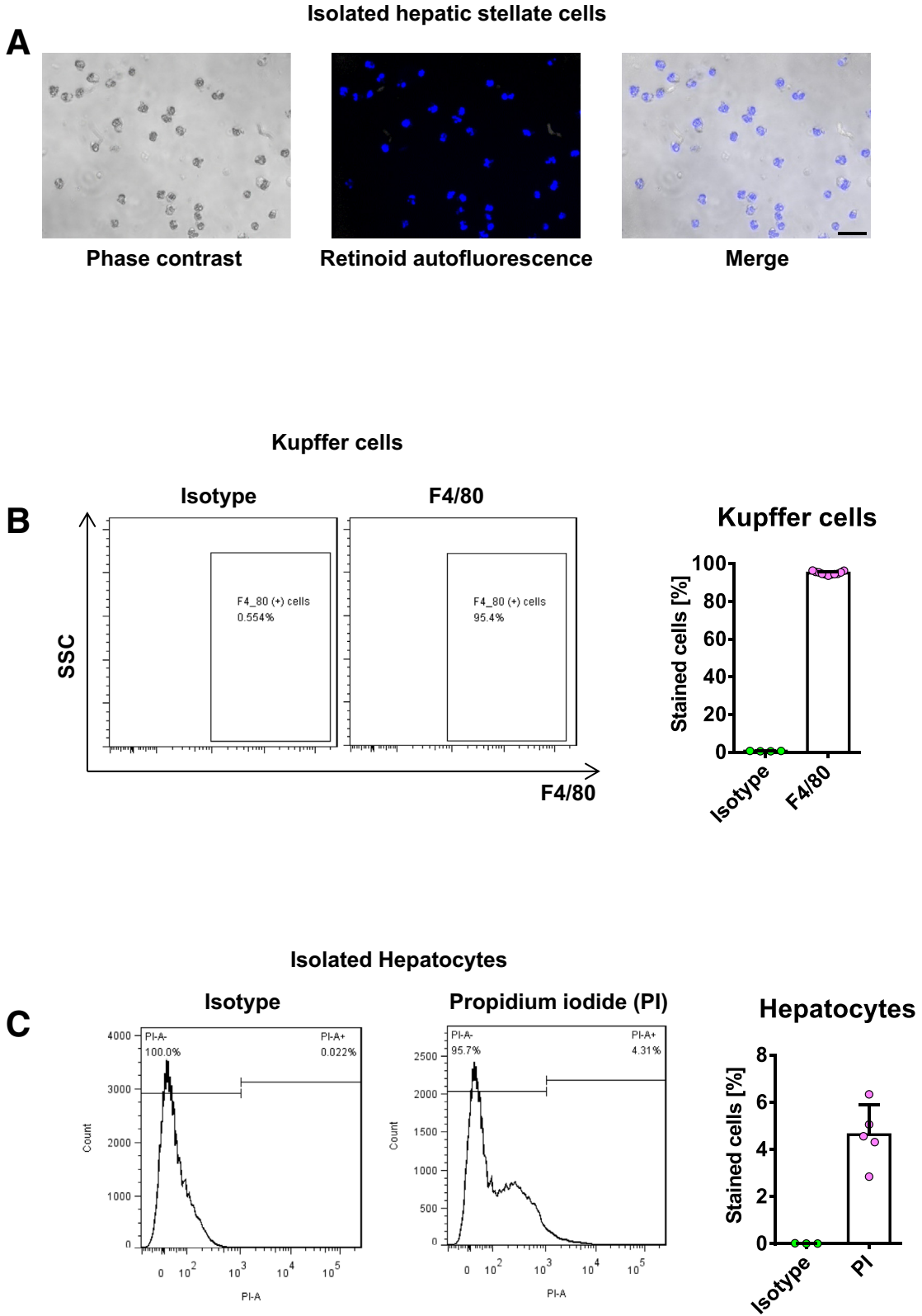


**Figure 17. Purity and viability of primary liver cells.** (A) Purity of the HSCs was assessed by retinoid autofluorescence. Freshly isolated HSCs from normal mice were visualized under phase-contrast microscopy and retinoid fluorescence. Scale bar: 50  $\mu$ m. (B) Purity of the KCs was confirmed by flow cytometry for F4/80 expression. (C) Viability of hepatocytes after 24 hours in culture was assessed by flow cytometric analysis of propidium iodide expression.

Kupffer cells were positively selected as F4/80-expressing cells using magnetic-activated cell sorting (Miltenyi Biotec, GmbH, Bergisch Gladbach, Germany).<sup>43</sup> The procedure led to the isolation of KCs with 95% purity that was confirmed by flow cytometry for F4/80 expression (Figure 17B). To investigate the effect of LPS on PRR expression,  $3 \times 10^5$  KCs were plated in 6-well plates in RPMI-1640 in the presence of LPS (100 ng/mL; Sigma-Aldrich, Inc, St. Louis, MO) or vehicle for 24 hours. Sinusoidal endothelial cells were isolated using magnetic-activated cell sorting-based positive selection using CD31-specific antibodies (Miltenyi Biotec).

Primary hepatocytes were isolated from male C57BL/6 mice by modifying a previously described collagenase perfusion method.<sup>44</sup> The viability of hepatocytes after 24 hours in culture was >95%, as assessed by flow cytometry after propidium iodide staining (Figure 17C). Cell culture plates were coated with 0.1% rat tail collagen (Sigma-Aldrich) 24 hours before plating the cells. Collagenases D and P were purchased from Roche (Mannheim, Germany). Primary hepatocytes were plated in 6-well plates ( $2 \times 10^5$  cells/well) and cultured in DMEM containing 10% FBS and antibiotics at 37°C in a humidified atmosphere of 95% air and 5% CO<sub>2</sub>. RNA was extracted after 24 hours of culture.

### Measurement of Blood Biochemistry

Serum ALT levels were measured with a standard auto-SMAC analyzer (Cobas 8000; Roche Diagnostics GmbH, Mannheim, Germany).

### Real-Time Quantitative Reverse Transcriptase PCR

Nucleotide sequences of the primers used in this study are shown in Table 2. Gene expression levels were measured quantitatively using an ABI PRISM 7900HT Sequence Detection System (Applied Biosystems, Inc, Foster City, CA) using SYBR Green. The specificity of each PCR product was evaluated by melting curve analysis, followed by agarose gel electrophoresis.

Nested PCR analysis was used to detect hepatic Va14-Ja18 mRNA.<sup>45</sup> Briefly, first-round PCR was performed with the following primers: 5'-ATGAAAAGCGCCTGAGTGCC-3' and 5'-CAGGAGGATTCGGAGTCCCA-3' using the following cycling conditions: 40 cycles of 94°C for 1 minute, 53°C for 1 minute, and 72°C for 2 minutes. Five microliters of first-round PCR product were used to run in the nested PCR with the following primers: 5'-TAAGCACAGCACGTGCACAT-3' and 5'-CAATCAGCTGAGTCCCAGCT-3' using the following cycling conditions: 40 cycles of 94°C for 1 minute, 52°C for 1 minute, and 72°C for 2 minutes. The products were visualized and quantified on a 3% agarose gel.

### Western Blot Analysis

The blots were incubated with the primary antibodies shown in Table 3. After washing, the membranes were incubated with horseradish-peroxidase-conjugated goat anti-rabbit secondary antibodies (Jackson ImmunoResearch

Laboratories, Inc, West Grove, PA) for the rabbit primary antibodies for 1 hour. Subsequently, the blots were developed by enhanced chemiluminescence (ECL Western Blotting Analysis System, Amersham, Buckinghamshire, UK). The intensities of the bands of interest were analyzed using ImageJ software (National Institutes of Health, Bethesda, MD).

### Immunohistochemical Staining

Slides were incubated at 4°C overnight with the primary antibodies as shown in Table 3. After overnight incubation, the slides were incubated with the corresponding secondary antibody for 30 minutes. The slides were stained with a super-sensitive polymer-horseradish peroxidase immunohistochemistry detection system (BioGenex Laboratories, Inc, Fremont, CA) and then counterstained with Mayer's hematoxylin. Images were captured with a microscope (Olympus, AX-80, Tokyo, Japan) and Olympus Cell Sens imaging software.

### Immunofluorescence Staining

Liver sections were fixed with 4% paraformaldehyde and permeabilized with 0.1% Triton X-100 (Abcam, Cambridge, MA). On the first day of double staining, the sections were incubated with PRR and  $\alpha$ -SMA antibodies or GFP and  $\alpha$ -SMA antibodies (Table 3) for 16 hours at 4°C. Then, the sections were incubated with Alexa Fluor 488 donkey anti-sheep IgG H&L (ab150177; Abcam, Cambridge, MA) at a 1/1000 dilution for  $\alpha$ -SMA and Alexa Fluor 647 donkey anti-rabbit IgG H&L (ab150075; Abcam) at a 1/1000 dilution for PRR and GFP for 120 minutes at 37°C on day 2 and counterstained with 4', 6-diamidino-2-phenylindole (Cell Signaling).

### Sirius Red Staining

Sirius red staining was performed using the Sirius Red Staining Kit (Polysciences, Inc, Warrington, PA).

### Measurement of Hepatic Hydroxyproline and Triglyceride Levels

Hydroxyproline level was determined using a Hydroxyproline Colorimetric Assay Kit (BioVision, Inc). Liver tissue (20 mg) was homogenized and hydrolyzed with 200  $\mu$ L of 12 N HCl in a pressure-tight, Teflon-capped vial (Scientific Specialties, Inc, CA) at 120°C for 3 hours. After transferring 10  $\mu$ L of each hydrolyzed sample to a 96-well plate to dry at 65°C, 100  $\mu$ L of the chloramine T reagent was added to each sample, and the plate was incubated at 22°C–28°C for 5 minutes. After adding 100  $\mu$ L of the 4-(dimethylamino) benzaldehyde (DMAB) reagent to each well and incubating for 90 minutes at 60°C, the absorbance of all samples was measured at 560 nm using a microplate reader. Hepatic levels of triglyceride were measured using the Triglyceride Liquid Reagents Kit (Pointe Scientific, Canton, MI).

**Table 2.** Primers Used for Quantitative Reverse-Transcription PCR

Gene name	Primer	Sequence	Size, bp
<b>Mouse</b>			
Atp6ap2 (PRR)	Forward	5'-GCCAGGAGAGAGTGTATA-3'	145
	Reverse	5'-TCATTATTCCTACTCAGAG-3'	
Tgfb1	Forward	5'-GTGGAAATCAACGGGATCAG-3'	229
	Reverse	5'-ACTTCCAACCCAGGTCTTC-3'	
Serpine1 (PAI-1)	Forward	5'-GCCAGGGTTGCACTAACAT-3'	147
	Reverse	5'-GCCTCCTCATCCTGCCTAA-3'	
Fn1	Forward	5'-GTGGCTGCCTTCAACTTTC-3'	132
	Reverse	5'-GTGGGTTGCAAACCTTCAAT-3'	
Ccl2	Forward	5'-ATTGGGATCATCTTGCTGGT-3'	108
	Reverse	5'-CCTGCTGTTACAGTTGCC-3'	
Acta2	Forward	5'-GTCCAGACATCAGGGAGTAA-3'	102
	Reverse	5'-TCGGATACTTCAGCGTCAGGA-3'	
Col1a1	Forward	5'-GAGCGGAGAGTACTGGATCG-3'	158
	Reverse	5'-GCTTCTTTTCTTGGGGTTC-3'	
Timp1	Forward	5'-TGGGGAACCCATGAATTTAG-3'	127
	Reverse	5'-ATCTGGCATCCTCTTGTGCA-3'	
Ptgs2 (COX-2)	Forward	5'-CAGACAACATAAACTGCGCCTT-3'	71
	Reverse	5'-GATACACCTCTCCACCAATGACC-3'	
Il1b	Forward	5'-GAACCAAGCAACGACAAA-3'	197
	Reverse	5'-GCAGACTCAAATCCACT-3'	
Tnf	Forward	5'-TGCTATGTCTCAGCCTCTC-3'	117
	Reverse	5'-GAGGCCATTTGGGAACCTTCT-3'	
Il6	Forward	5'-CTCTGGGAAATCGTGGAAAT-3'	134
	Reverse	5'-CCAGTTTGGTAGCATCCA TCA-3'	
Renin	Forward	5'-GAGGCCTTCCTTGACCAATC-3'	188
	Reverse	5'-TGTGAATCCCAAGCAAGG-3'	
Gapdh	Forward	5'-TGTTGAAGTCGCAGGAGACAACCT-3'	111
	Reverse	5'-AACCTGCCAAGTATGATGACATCA-3'	
<b>Human</b>			
TGFB1	Forward	5'-CCCAGCATCTGCAAAGCTC-3'	101
	Reverse	5'-GTCAATGTACAGCTGCCGCA-3'	
SERPINE1	Forward	5'-AGTCCTTGTACAGATGCCG-3'	101
	Reverse	5'-ACAACAGGAGGAAACCCA-3'	
FN1	Forward	5'-ACCTCGGTGTTGTAAGGTGG-3'	91
	Reverse	5'-CCATAAAGGGCAACCAAGAG-3'	
<b>Human</b>			
ACTA2	Forward	5'-AGGCACCCCTGAACCCCAA-3'	101
	Reverse	5'-CAGCACCGCCTGGATAGCC-3'	
COL1A1	Forward	5'-AACATGACCAAAAACAAAAGTG-3'	252
	Reverse	5'-CATTGTTTCTGTGTCTTCTGG-3'	
TIMP1	Forward	5'-AGACGGCCTTCTGCAATTCC-3'	84
	Reverse	5'-GCTGGTATAAGTGGTCTGGTT-3'	
PTGS2	Forward	5'-CCGGGTACAATCGCAATTAT-3'	103
	Reverse	5'-GGCGCTCAGCCATACAG-3'	
GAPDH	Forward	5'-CACACGTCTCGGTATGGTA-3'	155
	Reverse	5'-AAGAGGAAGGCCAAGTCGAG-3'	

COX-2, cyclooxygenase-2; GAPDH, glyceraldehyde-3-phosphate dehydrogenase.

### Flow Cytometry

The mouse-specific antibodies used are shown in [Table 3](#). Mouse fragment crystallizable (Fc) block (eBioscience, San Diego, CA) was used to block binding of aggregated immunoglobulins to Fc receptors. Flow cytometry was performed on a FACSCanto II cytometer (BD Biosciences, San Jose, CA).

### In Vitro siRNA Transfection

To silence PRR expression in RAW 264.7 cells, specific mouse siRNAs (Santa Cruz Biotechnology, Inc, Paso Robles, CA) were used for transfection using Lipofectamine RNAiMAX (Thermo Fisher Scientific, Waltham, MA) following the manufacturer's instructions. Briefly, siRNA and Lipofectamine RNAiMAX were mixed and incubated at

**Table 3.** Antibody Details and Conditions Used for Western Blot and Immunostaining

Antibody	Supplier	Catalog no.	Application	Dilution
$\beta$ -actin	GeneTex (Irvine, CA)	GTX629630	WB	1:5000
GAPDH	Novus (Littleton, CO)	NB300-221	WB	1:1000
$\alpha$ -SMA	GeneTex	GTX100034	WB	1:1000
	Novus	NB300-978	IHC IF	1:2000 1:100
p-ERK1/2	Cell Signaling	9101	WB	1:1000
t-ERK1/2	Cell Signaling	9102	WB	1:1000
PRR	Santa Cruz	sc-67390	WB	1:1000
			IHC	1:1000
			IF	1:100
TGF- $\beta$ 1	Abcam	ab92486	WB	1:1000
p-Smad3	Cell Signaling	9520	WB	1:1000
Smad3	Cell Signaling	9523	WB	1:1000
F4/80	Abcam	ab6640	IF	1:500
MPO	Abcam	ab9535	IHC	1:50
GFP	GeneTex	GTX113617	IHC	1:1000
			IF	1:100
NKp46	R&D Systems	KWW0519071	IHC	1:50
His	Cell Signaling	12698	WB	1:1000
			FCM	1:800
(Pro)renin receptor	Everest Biotech (Ramona, CA)	EB06118	FCM	1:50
F4/80	Miltenyi Biotec	130-110-443	FCM	1:100
Propidium iodide	BioLegend	421301	FCM	1:20

FCM, flow cytometry; IF, immunofluorescence; IHC, immunohistochemistry; GAPDH, glyceraldehyde-3-phosphate dehydrogenase; NKp46, ; p-ERK1/2, phosphorylated extracellular signal regulated kinase 1/2; p-Smad3, phosphorylated Smad3; t-ERK1/2, total extracellular signal regulated kinase 1/2; WB, Western blot.

22°C–28°C for 5 minutes in Opti-MEM medium (Thermo Fisher Scientific, Waltham, MA). Then, the mixture was transferred to a 6-well plate at a final concentration of 20 nmol/L (siRNA) and 7.5  $\mu$ L RNAiMAX per well. Cells were assayed 48 hours after siRNA transfection, and the protein levels of PRR were evaluated using  $\beta$ -actin as a loading control. To test the effect of PRR knockdown on LPS-induced proinflammatory cytokines and chemokine expression, cells were treated with LPS (100 ng/mL; Sigma) for 24 hours for analysis of mRNA at 48 hours after siRNA transfection.

### Statistical Analysis

Data were analyzed using GraphPad Prism 8 (GraphPad Software, San Diego, CA) and are expressed as means  $\pm$  SD. Statistical significance between groups was determined using the nonparametric Mann–Whitney *U* test (2 groups) or Kruskal–Wallis tests followed by the Dunn tests (>2 groups). Significance was determined at *P* < .05.

### References

- Schuppan D, Afdhal NH. Liver cirrhosis. *Lancet* 2008; 371:838–851.
- Battaller R, Brenner DA. Liver fibrosis. *J Clin Invest* 2005; 115:209–218.
- Friedman SL. Mechanisms of hepatic fibrogenesis. *Gastroenterology* 2008;134:1655–1669.
- Schuppan D, Ashfaq-Khan M, Yang AT, Kim YO. Liver fibrosis: direct antifibrotic agents and targeted therapies. *Matrix Biol* 2018;68–69:435–451.
- Guicciardi ME, Gores GJ. Apoptosis: a mechanism of acute and chronic liver injury. *Gut* 2005;54:1024–1033.
- Lemoinne S, Friedman SL. New and emerging antifibrotic therapeutics entering or already in clinical trials in chronic liver diseases. *Curr Opin Pharmacol* 2019; 49:60–70.
- Nguyen G, Delarue F, Burcklé C, Bouzahir L, Giller T, Sraer J-D. Pivotal role of the renin/prorenin receptor in angiotensin II production and cellular responses to renin. *J Clin Invest* 2002;109:1417–1427.
- Nguyen G, Muller DN. The biology of the (pro)renin receptor. *J Am Soc Nephrol* 2010;21:18–23.
- Huang Y, Noble NA, Zhang J, Xu C, Border WA. Renin-stimulated TGF- $\beta$ 1 expression is regulated by a mitogen-activated protein kinase in mesangial cells. *Kidney Int* 2007;72:45–52.
- Huang Y, Wongamorntham S, Kasting J, McQuillan D, Owens RT, Yu L, Noble NA, Border W. Renin increases

- mesangial cell transforming growth factor-beta1 and matrix proteins through receptor-mediated, angiotensin II-independent mechanisms. *Kidney Int* 2006; 69:105–113.
11. Ichihara A, Kaneshiro Y, Takemitsu T, Sakoda M, Suzuki F, Nakagawa T, Nishiyama A, Inagami T, Hayashi M. Nonproteolytic activation of prorenin contributes to development of cardiac fibrosis in genetic hypertension. *Hypertension* 2006;47:894–900.
  12. Narumi K, Sato E, Hirose T, Yamamoto T, Nakamichi T, Miyazaki M, Sato H, Ito S. (Pro)renin receptor is involved in mesangial fibrosis and matrix expansion. *Sci Rep* 2018;8:16.
  13. Fellmann C, Hoffmann T, Sridhar V, Hopfgartner B, Muhar M, Roth M, Lai DY, Barbosa IA, Kwon JS, Guan Y, Sinha N, Zuber J. An optimized microRNA backbone for effective single-copy RNAi. *Cell Rep* 2013;5:1704–1713.
  14. Jimenez Calvente C, Sehgal A, Popov Y, Kim YO, Zevallos V, Sahin U, Diken M, Schuppan D. Specific hepatic delivery of procollagen alpha1(I) small interfering RNA in lipid-like nanoparticles resolves liver fibrosis. *Hepatology* 2015;62:1285–1297.
  15. Sato Y, Murase K, Kato J, Kobune M, Sato T, Kawano Y, Takimoto R, Takada K, Miyanishi K, Matsunaga T, Takayama T, Niitsu Y. Resolution of liver cirrhosis using vitamin A-coupled liposomes to deliver siRNA against a collagen-specific chaperone. *Nat Biotechnol* 2008; 26:431–442.
  16. Ramkumar N, Kohan DE. The (pro)renin receptor: an emerging player in hypertension and metabolic syndrome. *Kidney Int* 2019;95:1041–1052.
  17. Ichihara A, Hayashi M, Kaneshiro Y, Suzuki F, Nakagawa T, Tada Y, Koura Y, Nishiyama A, Okada H, Uddin MN, Nabi AHMN, Ishida Y, Inagami T, Saruta T. Inhibition of diabetic nephropathy by a decoy peptide corresponding to the “handle” region for nonproteolytic activation of prorenin. *J Clin Invest* 2004; 114:1128–1135.
  18. Muller DN, Klanke B, Feldt S, Cordasic N, Hartner A, Schmieder RE, Luft FC, Hilgers KF. (Pro)renin receptor peptide inhibitor “handle-region” peptide does not affect hypertensive nephrosclerosis in Goldblatt rats. *Hypertension* 2008;51:676–681.
  19. Feldt S, Maschke U, Dechend R, Luft FC, Muller DN. The putative (pro)renin receptor blocker HRP fails to prevent (pro)renin signaling. *J Am Soc Nephrol* 2008; 19:743–748.
  20. te Riet L, van den Heuvel M, Peutz-Kootstra CJ, van Esch JH, van Veghel R, Garrelds IM, Musterd-Bhaggoe U, Bouhuizen AM, Leijten FP, Danser AH, Batenburg WW. Deterioration of kidney function by the (pro)renin receptor blocker handle region peptide in aliskiren-treated diabetic transgenic (mRen2)27 rats. *Am J Physiol Renal Physiol* 2014;306:F1179–F1189.
  21. Campbell DJ. Critical review of prorenin and (pro)renin receptor research. *Hypertension* 2008;51:1259–1264.
  22. Sakoda M, Ichihara A, Kaneshiro Y, Takemitsu T, Nakazato Y, Nabi AH, Nakagawa T, Suzuki F, Inagami T, Itoh H. (Pro)renin receptor-mediated activation of mitogen-activated protein kinases in human vascular smooth muscle cells. *Hypertens Res* 2007; 30:1139–1146.
  23. Bataller R, Sancho-Bru P, Gines P, Lora JM, Al-Garawi A, Sole M, Colmenero J, Nicolas JM, Jimenez W, Weich N, Gutierrez-Ramos JC, Arroyo V, Rodes J. Activated human hepatic stellate cells express the renin-angiotensin system and synthesize angiotensin II. *Gastroenterology* 2003;125:117–125.
  24. Asbert M, Jimenez W, Gaya J, Gines P, Arroyo V, Rivera F, Rodes J. Assessment of the renin-angiotensin system in cirrhotic patients. Comparison between plasma renin activity and direct measurement of immunoreactive renin. *J Hepatol* 1992;15:179–183.
  25. Inagaki Y, Okazaki I. Emerging insights into transforming growth factor beta Smad signal in hepatic fibrogenesis. *Gut* 2007;56:284–292.
  26. Schnabl B, Kweon YO, Frederick JP, Wang XF, Rippe RA, Brenner DA. The role of Smad3 in mediating mouse hepatic stellate cell activation. *Hepatology* 2001; 34:89–100.
  27. Li Z, Zhou L, Wang Y, Miao J, Hong X, Hou FF, Liu Y. (Pro)renin receptor is an amplifier of Wnt/beta-catenin signaling in kidney injury and fibrosis. *J Am Soc Nephrol* 2017;28:2393–2408.
  28. Gonzalez AA, Zamora L, Reyes-Martinez C, Salinas-Parra N, Roldan N, Cuevas CA, Figueroa S, Gonzalez-Vergara A, Prieto MC. (Pro)renin receptor activation increases profibrotic markers and fibroblast-like phenotype through MAPK-dependent ROS formation in mouse renal collecting duct cells. *Clin Exp Pharmacol Physiol* 2017;44:1134–1144.
  29. Huang J, Siragy HM. Glucose promotes the production of interleukin-1beta and cyclooxygenase-2 in mesangial cells via enhanced (Pro)renin receptor expression. *Endocrinology* 2009;150:5557–5565.
  30. Kanda A, Ishizuka ET, Shibata A, Matsumoto T, Toyofuku H, Noda K, Namba K, Ishida S. A novel single-strand RNAi therapeutic agent targeting the (pro)renin receptor suppresses ocular inflammation. *Mol Ther Nucleic Acids* 2017;7:116–126.
  31. Ren L, Sun Y, Lu H, Ye D, Han L, Wang N, Daugherty A, Li F, Wang M, Su F, Tao W, Sun J, Zelcer N, Mullick AE, Danser AHJ, Jiang Y, He Y, Ruan X, Lu X. (Pro)renin receptor inhibition reprograms hepatic lipid metabolism and protects mice from diet-induced obesity and hepato-steatosis. *Circ Res* 2018;122:730–741.
  32. Gayban AJB, Worker CJ, Anakatumpunya T, Earley YF. (Pro)renin receptor antagonism attenuates high fat diet induced non-alcoholic fatty liver disease. *FASEB* 2020. <https://doi.org/10.1096/fasebj.2020.34.s1.06020>.
  33. Asai A, Chou PM, Bu HF, Wang X, Rao MS, Jiang A, DiDonato CJ, Tan XD. Dissociation of hepatic insulin resistance from susceptibility of nonalcoholic fatty liver disease induced by a high-fat and high-carbohydrate diet in mice. *Am J Physiol Gastrointest Liver Physiol* 2014;306:G496–G504.
  34. Angulo P, Kleiner DE, Dam-Larsen S, Adams LA, Bjornsson ES, Charatcharoenwitthaya P, Mills PR, Keach JC, Lafferty HD, Stahler A, Haffladottir S, Bendtsen F. Liver fibrosis, but no other histologic

- features, is associated with long-term outcomes of patients with nonalcoholic fatty liver disease. *Gastroenterology* 2015;149:389–397 e10.
35. Son G, Hines IN, Lindquist J, Schrum LW, Rippe RA. Inhibition of phosphatidylinositol 3-kinase signaling in hepatic stellate cells blocks the progression of hepatic fibrosis. *Hepatology* 2009;50:1512–1523.
  36. Strnad P, Tao GZ, Zhou Q, Harada M, Toivola DM, Brunt EM, Omary MB. Keratin mutation predisposes to mouse liver fibrosis and unmasks differential effects of the carbon tetrachloride and thioacetamide models. *Gastroenterology* 2008;134:1169–1179.
  37. Koo JH, Lee HJ, Kim W, Kim SG. Endoplasmic reticulum stress in hepatic stellate cells promotes liver fibrosis via PERK-mediated degradation of HNRNPA1 and up-regulation of SMAD2. *Gastroenterology* 2016;150:181–193 e8.
  38. Themis M, Forbes SJ, Chan L, Cooper RG, Etheridge CJ, Miller AD, Hodgson HJ, Coutelle C. Enhanced in vitro and in vivo gene delivery using cationic agent complexed retrovirus vectors. *Gene Ther* 1998;5:1180–1186.
  39. Xu C, Zhang M, Li K, Ni M, Bai Y, Zhang J, Song X, Wang J. CD24(hi)CD38(hi) B regulatory cells from patients with end plate inflammation presented reduced functional potency. *Int Immunopharmacol* 2019;70:295–301.
  40. Lee KC, Hsieh YC, Chan CC, Sun HJ, Huang YH, Hou MC, Lin HC. Human relaxin-2 attenuates hepatic steatosis and fibrosis in mice with non-alcoholic fatty liver disease. *Lab Invest* 2019;99:1203–1216.
  41. Iwaisako K, Haimerl M, Paik Y-H, Taura K, Kodama Y, Sirlin C, Yu E, Yu RT, Downes M, Evans RM, Brenner DA, Schnabl B. Protection from liver fibrosis by a peroxisome proliferator-activated receptor  $\delta$  agonist. *Proc Natl Acad Sci U S A* 2012;109:E1369.
  42. Mederacke I, Dapito DH, Affo S, Uchinami H, Schwabe RF. High-yield and high-purity isolation of hepatic stellate cells from normal and fibrotic mouse livers. *Nat Protoc* 2015;10:305–315.
  43. Seki E, De Minicis S, Osterreicher C, Kluwe J, Osawa Y, Brenner D, Schwabe R. TLR4 enhances TGF-beta signaling and hepatic fibrosis. *Nat Med* 2007;13:1324–1332.
  44. Severgnini M, Sherman J, Sehgal A, Jayaprakash NK, Aubin J, Wang G, Zhang L, Peng CG, Yucius K, Butler J, Fitzgerald K. A rapid two-step method for isolation of functional primary mouse hepatocytes: cell characterization and asialoglycoprotein receptor based assay development. *Cytotechnology* 2012;64:187–195.
  45. Lee KC, Chen P, Maricic I, Inamine T, Hu J, Gong S, Sun JC, Dasgupta S, Lin HC, Lin YT, Loomba R, Starkel P, Kumar V, Schnabl B. Intestinal iNKT cells migrate to liver and contribute to hepatocyte apoptosis during alcoholic liver disease. *Am J Physiol Gastrointest Liver Physiol* 2019;316:G585–G597.

---

Received December 17, 2020. Accepted May 25, 2021.

#### Correspondence

Address correspondence to: Kuei-Chuan Lee, MD, PhD, Division of Gastroenterology and Hepatology, Department of Medicine, Taipei Veterans General Hospital, 201, Section 2, Shih-Pai Road, Taipei 11217, Taiwan. e-mail: kcleee2@vghtpe.gov.tw; fax: (886) 2-2873-9318.

#### Acknowledgments

The authors thank Ms Hsiu-Ying Chen and Ms Fu-Jung Shou for their excellent technical assistance and would like to acknowledge the support of the Biobank of Taipei Veterans General Hospital, the National Institutes of Diabetes and Digestive and Kidney Diseases-funded San Diego Digestive Diseases Research Center (P30 DK120515), and the National RNAi Core Facility at Academia Sinica in Taiwan.

#### CRedit Authorship Contributions

Yun-Cheng Hsieh, MD (Formal analysis: Lead; Investigation: Lead; Writing – original draft: Equal)  
 Kuei-Chuan Lee, MD, PhD (Conceptualization: Lead; Formal analysis: Lead; Supervision: Lead; Writing – original draft: Equal)  
 Hao-Jan Lei, MD (Resources: Supporting)  
 Keng-Hsin Lan, MD, PhD (Investigation: Supporting; Methodology: Supporting)  
 Teh-Ia Huo, MD (Investigation: Supporting)  
 Yi-Tsung Lin, MD, PhD (Formal analysis: Supporting; Methodology: Supporting)  
 Che-Chang Chan, MD, PhD (Formal analysis: Supporting; Methodology: Supporting)  
 Bernd Schnabl, MD (Formal analysis: Supporting)  
 Yi-Hsiang Huang, MD, PhD (Investigation: Supporting)  
 Ming-Chih Hou, MD (Investigation: Supporting)  
 Han-Chieh Lin, MD (Investigation: Supporting)

#### Conflicts of interest

The authors disclose no conflicts.

#### Funding

This study was supported by grants from Taipei Veterans General Hospital (V108B-006) and the Ministry of Science and Technology, Taiwan (MOST 104-2314-B-075-023-MY2, 106-2314-B-075-005-MY2, 108-2628-B-075-008, and 109-2628-B-075-016).